Discrete phase shift analysis of π^+p scattering in Plab range 77-725 MeV/c (3-rd Iteration)

V.Abaev, P.Metsa, M.Sainio

26 June 2007

Abstract

The main goal is to improve the traditional Discrete Phase Shift Analysis and combine it with a different theoretical constraits followed from FDR, Zero Trajectories and PWDR.

1 Motivation

Since completion KH and CMU analyses there were no valuable global phase shift analyses in pion-nucleon scattering. There are at least 2 main reasons:

1. The loss of interest to pion-nucleon physics.
2. A huge efforts to execute analysis.

The majority in physical community are satisfied by a simple treatment of the Fermi series in partial wave parameter space. Just the trivial "student's" fitting of the data or oversimplified model-depended approaches. No headache but a lot of speculations around physics. This way was chosen by R.A. Arndt.

We are not satisfied in this situation and going to take into account all advantages of KH-CMU approaches, develope the new one and improve the Discrete Phase Shift Analysis Core as much as possible.

To be free from additional physical problems we have chosen the simplest case of π^+p scattering to test our code:

1. No problem with an isospin violation. Pure isospin 3/2 state.
2. There are no Discrete Ambiguities up to 750 MeV/c. Unique solution.
3. Existing EM Tromborg Correction.
4. The Data Base is not so big.

As a basic Code for improvement we have taken PNPI version of Discrete Phase Shift Analysis.

2 Problems

If to forget about qualified manpower and financial support one can define two classes of problems in practical phase shift analyses,- "Experimental" and "Theoretical". This subdivision is a little bit artificial but very important. The first kind is usually thoroughly hidden and out of discussions.

1. "Experimental".

   If to be honest and to calculate χ^2/Ndf or Confidence Level for any Phase Shift Analysis using the complete Data Base we'll see immediately that χ^2 is too large and CL goes to Zero. It means that the confidence of the analysis is negligiable and the results are absolutely unreliable.

   Other words the location of this analysis is in a waste-basket.

   The traditional solution of this problem is in a purifying of the Data Base. There are two aspects of this approach: external inconsistency between different experiments and internal inconsistency (bad χ^2 for some points in certain experiment). The both kinds of inconsistencies are terminated by very subjective and violent way: some expert's team just "recommended" to throw away certain experiments from the Data Base according to "4-star" classification.

   In spite of these efforts the CL of the data description still hasn't reliable level.

More then 10 years ago it was proposed new method of data analysis taking into account argument's errors and acceptances,- Argument Scaling Analysis. On this way the problem of inconsistency is resolving machinery in multi-dimensional space. We would follow it including in the analysis

(a) acceptances calculations and

(b) argument's uncertainties.

The first one means the smearing calculation of any observable over the experimental acceptances. It is very simple and very important where the observable has some structures. What we need is an additional experimental information.

The second one is also simple, but complicated. We have to introduce new set of parameters for every experiment and treat them as a constrained ones from the exepimental resolutions. Here we have to modify our code seriously. The effect of the argument scaling is very important not only where we have structures in the observables, but also where they are changing very fast in the argument's dimension.

For example let's look at the simplest case of π^+p total cross sections.

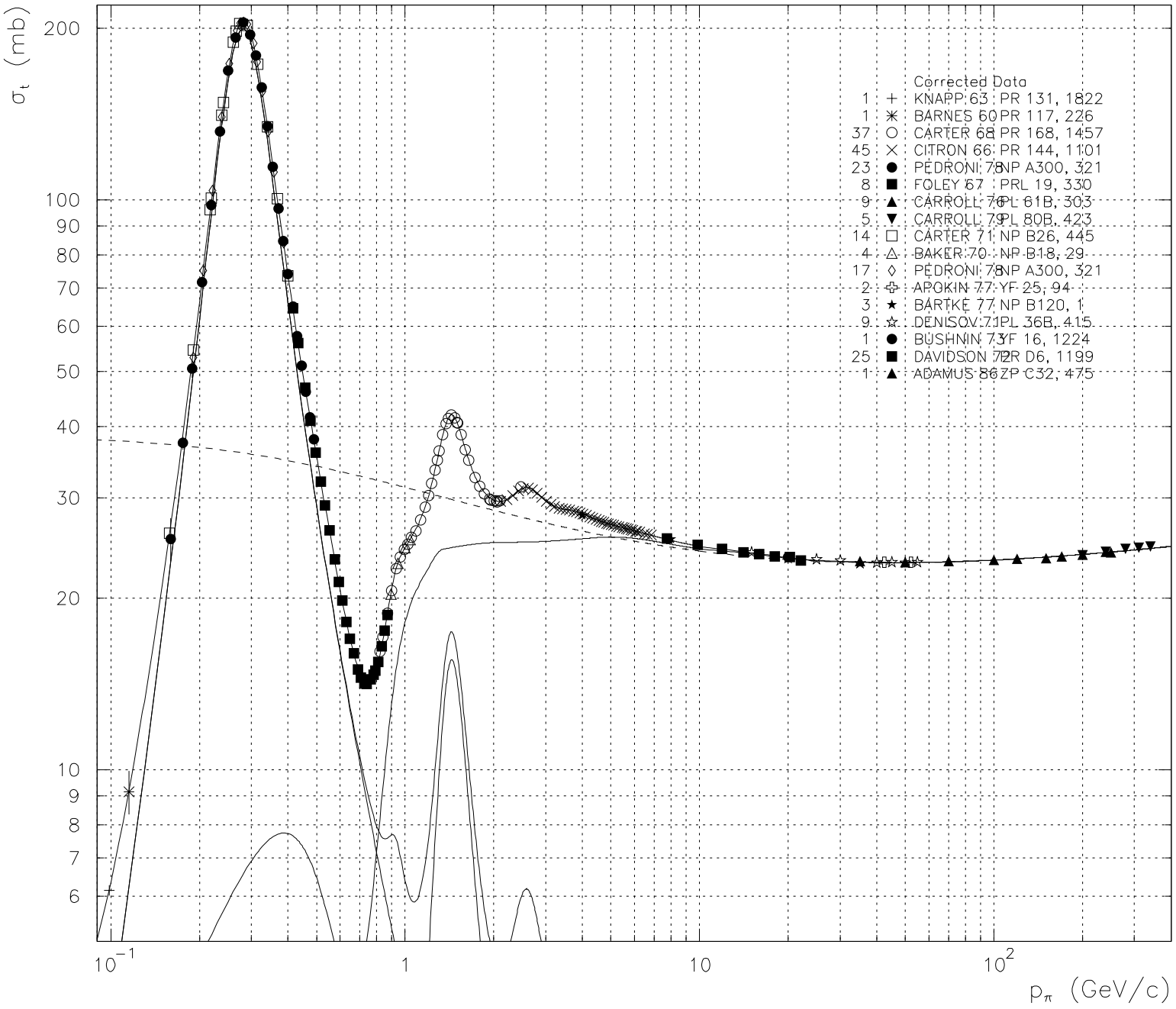

Figure 1: $\pi^+ p$ total cross sections.

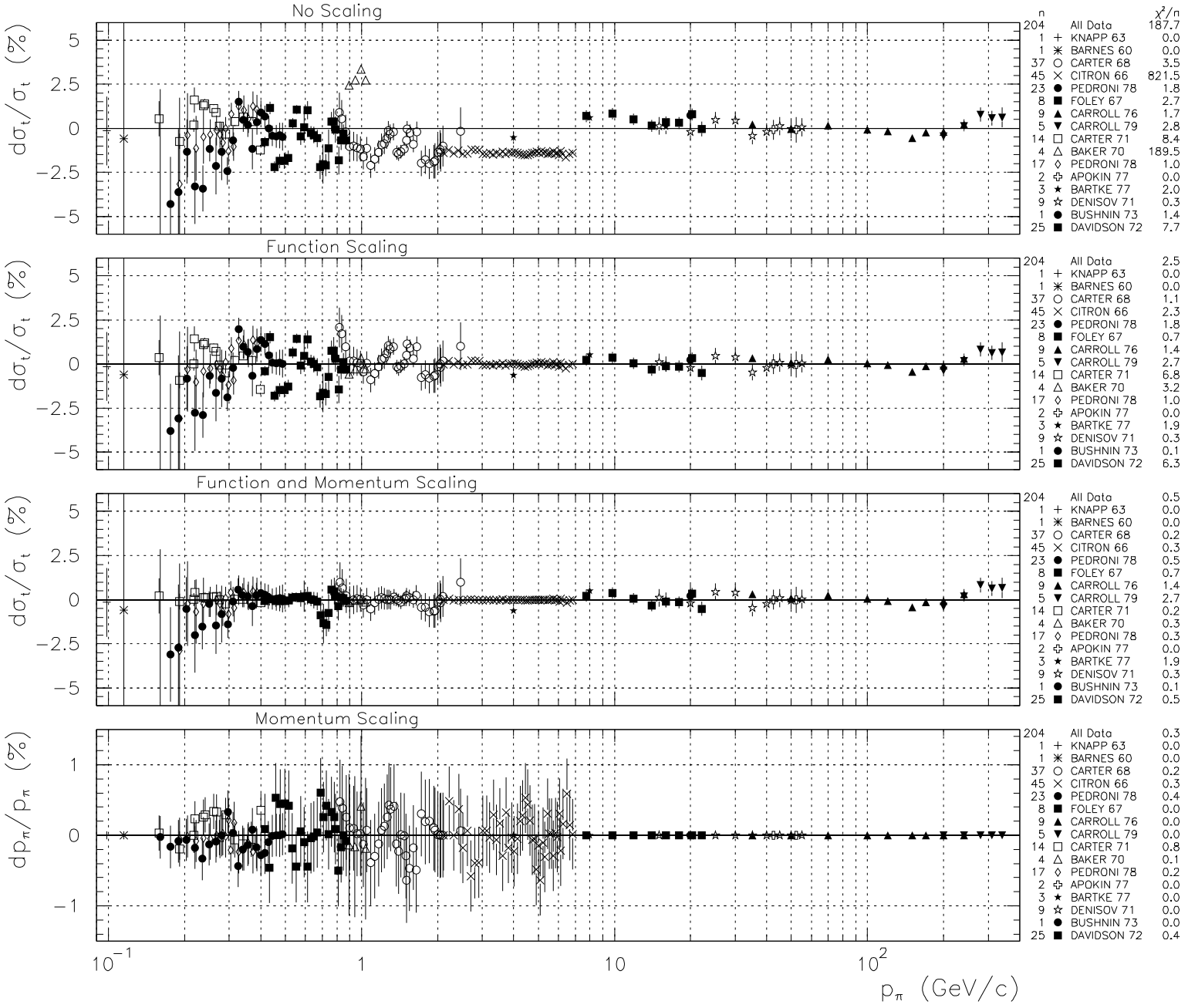

Figure 2: Deviation plots.

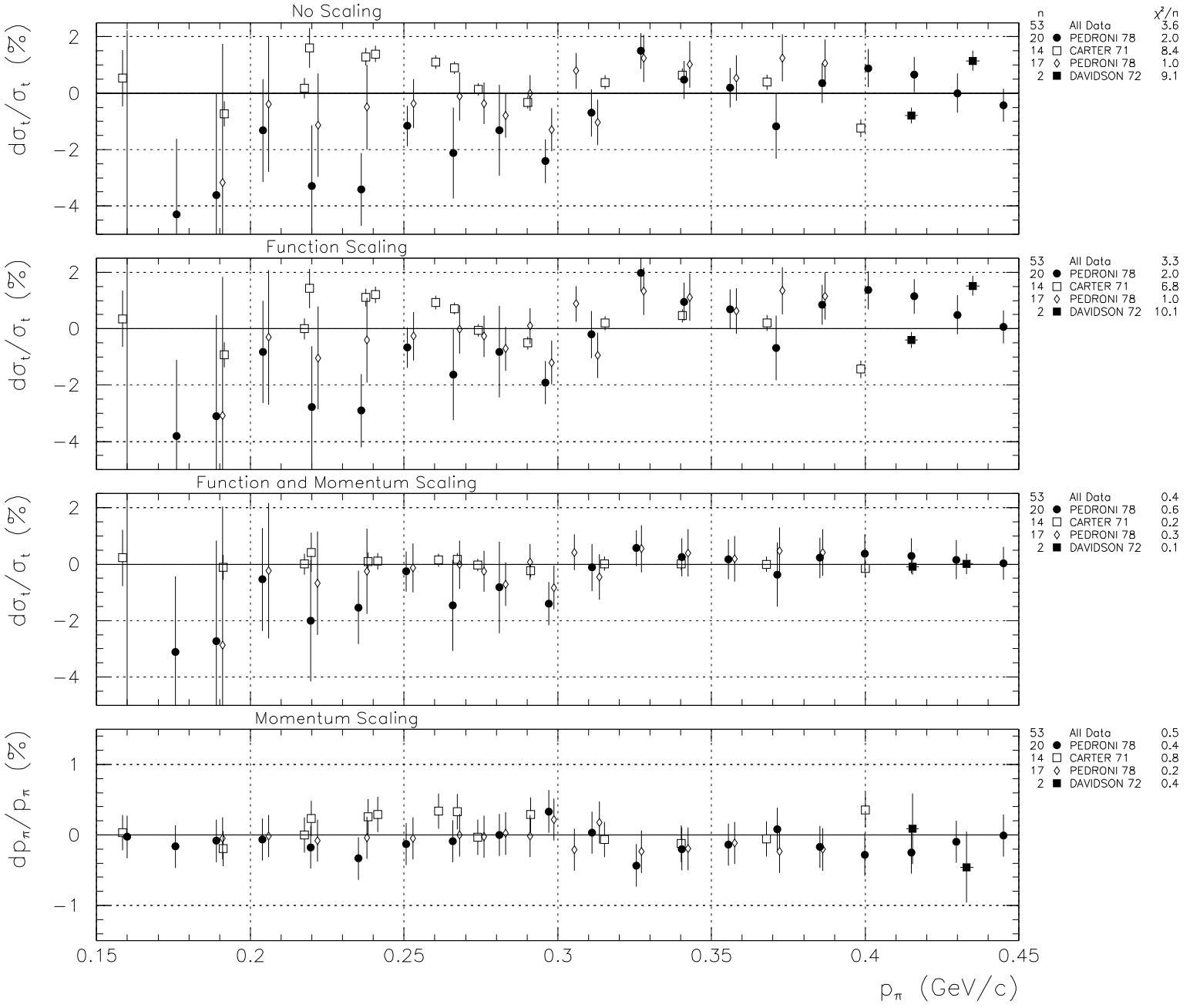

Figure 3: Deviation plots 150-450 MeV/c.

2. "Theoretical".

   There are some theoretical constraints which follow from the analyticity of the amplitudes and have to be included in the analysis. We have chosen the next ones:

   (a) FDR.

   They provide us the Real parts of the forward amplitudes from the interpolated total cross sections, "fixing" the forward point for differencial cross sections (hadronic). Both Real and Imaginary (total cross sections) parts are treated as "experimental" data as a result of interpolation for any momentum. In elastic region they are decreasing the correlation between phases extremely stong, because we know forward point and integral of the differential cross sections and the variations are responsible only for the shape of it.

   There are two ways how to calculate FDR:

   i. To take dispersion integral.

   ii. To use Pietarinen's expansion.

   We have chosen Pietarinen's approach and used it iteratively, spreading our momentum interval step by step. In detail this calculations will be given in report of Pekko Metsa.

   (b) PWDR.

   This dispersion relations help us to resolve the Cut-off problem. As an initial approach we have used the KH and PNPI results for the small amplitudes and extrapolated them to the threshold according to the effective-range approximation. This procedure was also iterative and gave us the tails of the high waves up to the threshold (H-wave approach). So, the small phases were treated under extrapolation constraints as an "experimental" ones. The phases more than 1^o were treated as a free parameters.

   (c) Zero Trajectories.

   Zero Trajectories formalism helps us not only to calculate any discrete abmiguities but can be used as a reflection of the analitic structure of the amplitude. For πN scattering if our amplitude

$$F(w) = \frac{F_o}{w^L} \prod_{i=1}^{2L} \frac{w - w_i}{1 - w_i} \qquad (1)$$
$$w = e^{i\Theta}, \qquad 0 \leq \Theta \leq 2\pi$$

   has two poles (say, nucleons) in s and u channels, then near the double pole

$$F \sim \frac{g^2}{s - m^2} + \frac{g^2}{u - m^2} = g^2 \frac{s + u - 2m^2}{(s - m^2)(u - m^2)}$$

we have a zero at $u = 2m^2 - s$, "double pole killing zero". Such zeros can propogate into physical region and we woud have zero for

$$\mid F(w) \mid^2 = \frac{d\sigma}{d\Omega}(1 \pm P)$$

or $P = \mp 1$ and minimums in differential cross section. Trajectories of these zeros can be analiticaly continued into any unphysical region. So, this alternative set of parameters, Zeros (w_i), is a good choice for analysis.

They can be expressed in terms of partial waves. Close to the threshold (L=1):

$$-\frac{2}{3}\frac{f_{o+}}{f_{1+}} = w_1 + w_2, \qquad 2\frac{f_{1-}}{f_{1+}} = 3w_1 w_2 - 1$$

$$w_{1,2} = \frac{-f_{0+} \pm \sqrt{f_{0+}^2 - 3f_{1+}^2 - 6f_{1-}f_{1+}}}{3f_{1+}}$$

and for $q \to 0$, $w_1 \to 0$, $w_2 \to -\frac{2}{3}\frac{f_{0+}}{f_{1+}} \to \infty$. This situation is general. When we are moving from the threshold, the Zeros are appearing by pairs from 0 and ∞ approaching the physical region. The parametrization of these trajectories can be used as a additional theoretical constraint to resolve the Cut-off problem.

Besides if to look at the formular(1) one can see that it is invariant for forward scattering amplitude in terms of zeros w_i. It means, varying zeros, the forward point and integral of the diffential cross sections are keeping the same. Only the shape is changing. And we can define the Zeros as a

$$w_i \equiv \quad Shape \quad Parameters.$$

It also can help us in analysis of the data, applying the smoothness on the variation in the shape of any observable.

There are some technical problems in practical application these Zero's properties in the Code. These problems are too special and can be omitted in this report. We did not resolve all of them up to now and hope to the next iteration this modification will be completed as an automated machinery code. But all Zeros were under the control and we have used them in some cases as an additional constraints.

Now let's look what we have with our Zeros and try to make some conclusions. Hope some of them will be surprising for You.

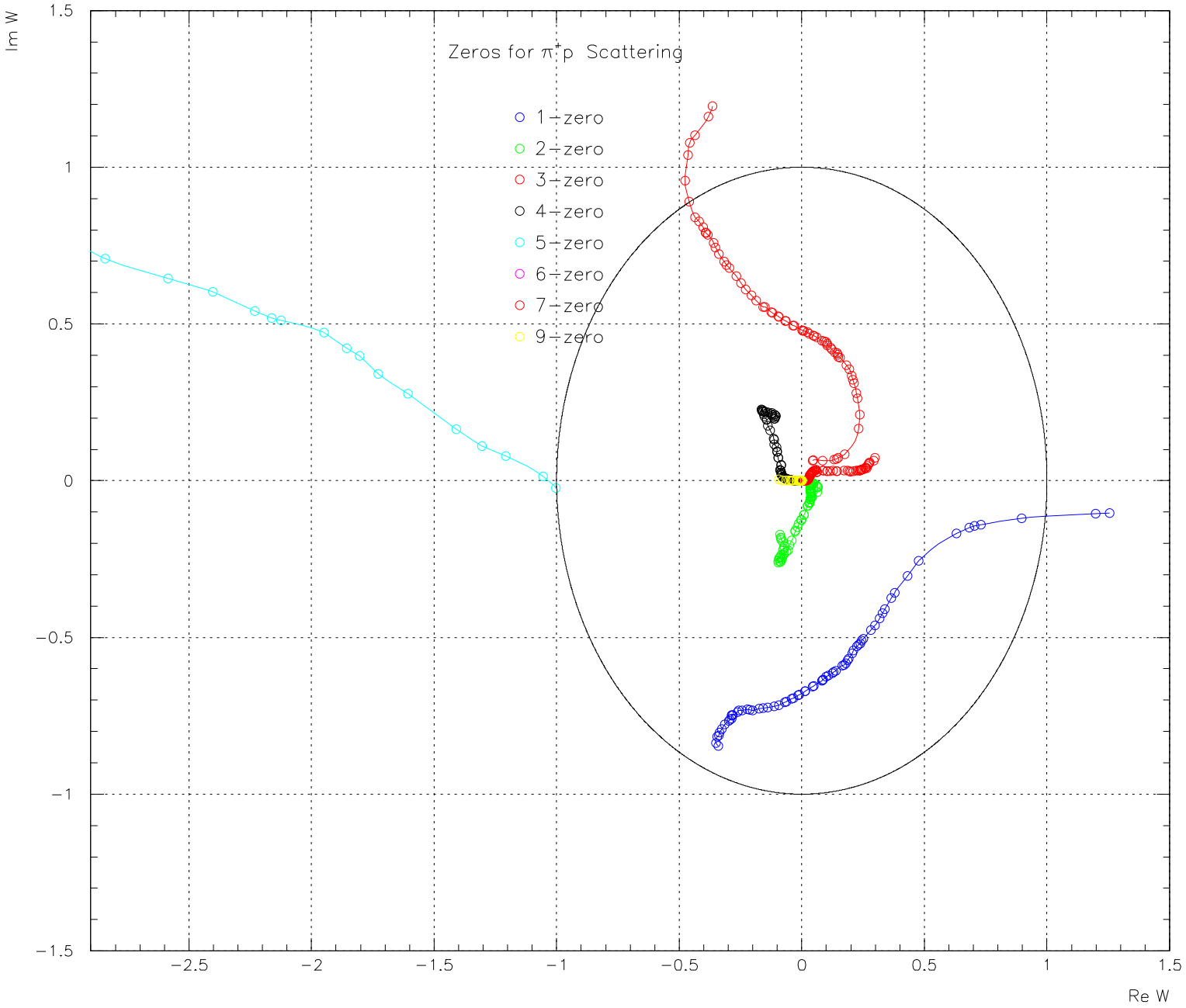

Figure 4: Zeros.

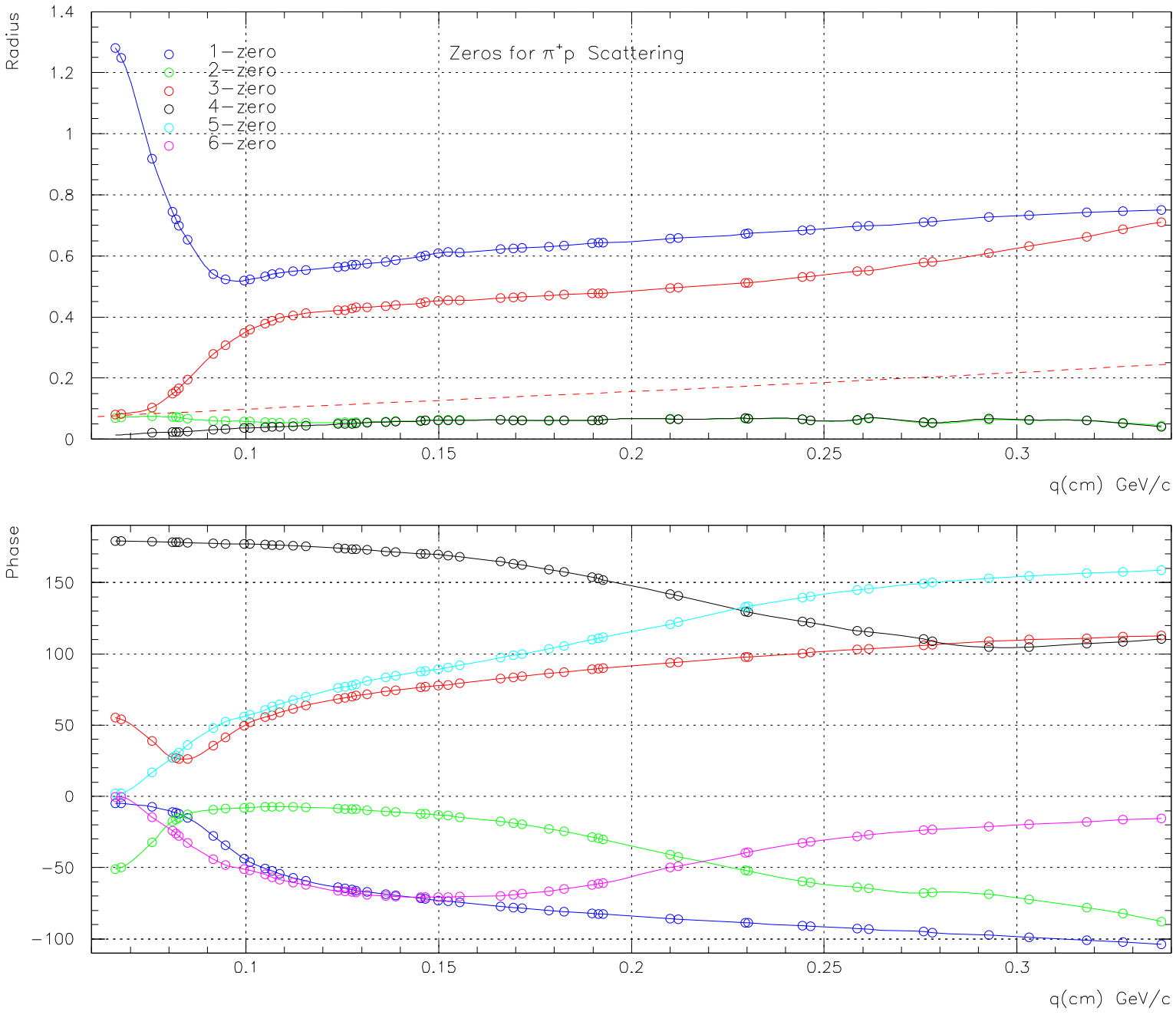

Figure 5: Radiuses and Phases(angles) of Zero Trajectories.

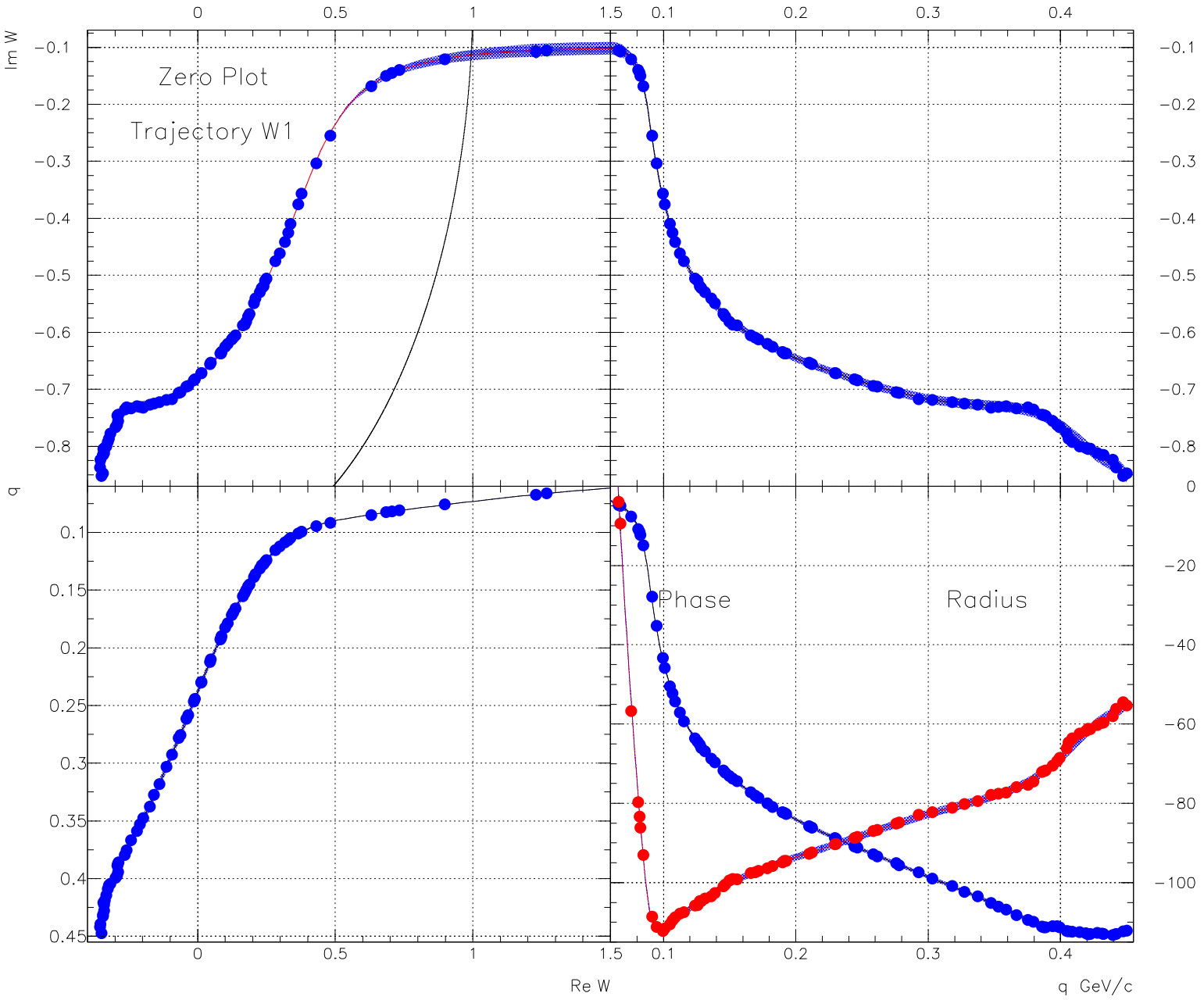

Figure 6: Zero Plot for Trajectory W1.

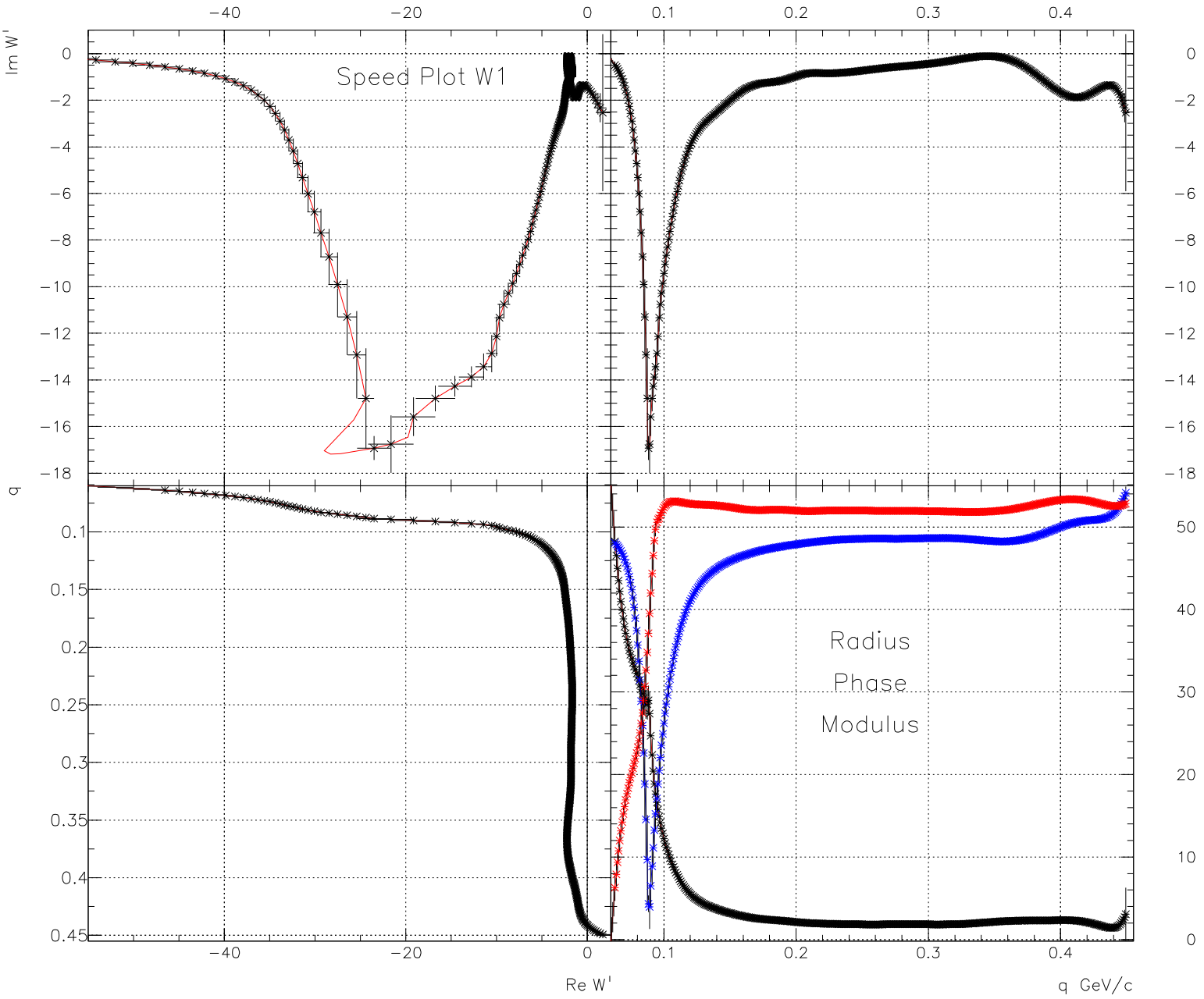

Figure 7: Zero Speed Plot fo Trajectory W1.

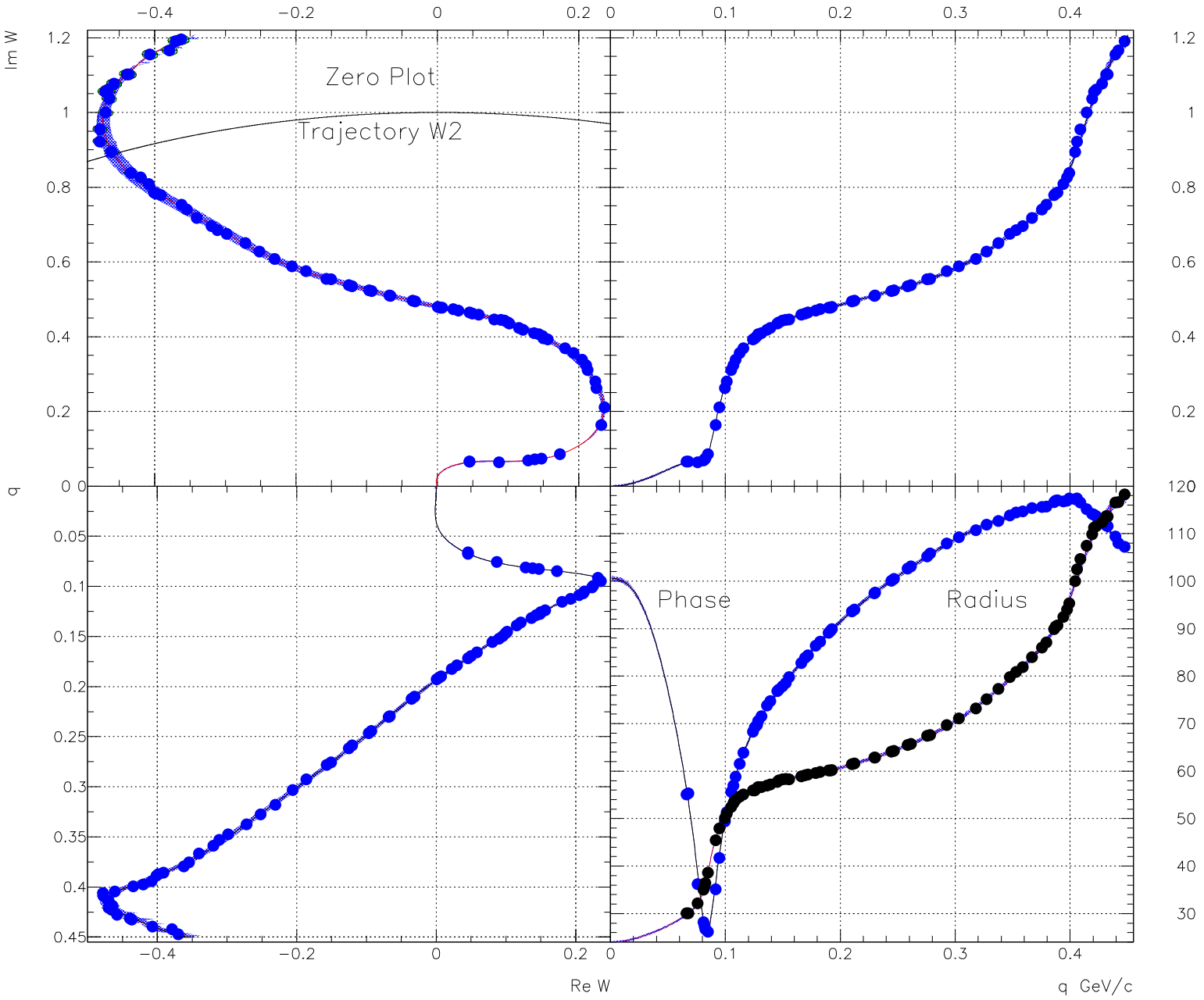

Figure 8: Zero Plot for Trajectory W2.

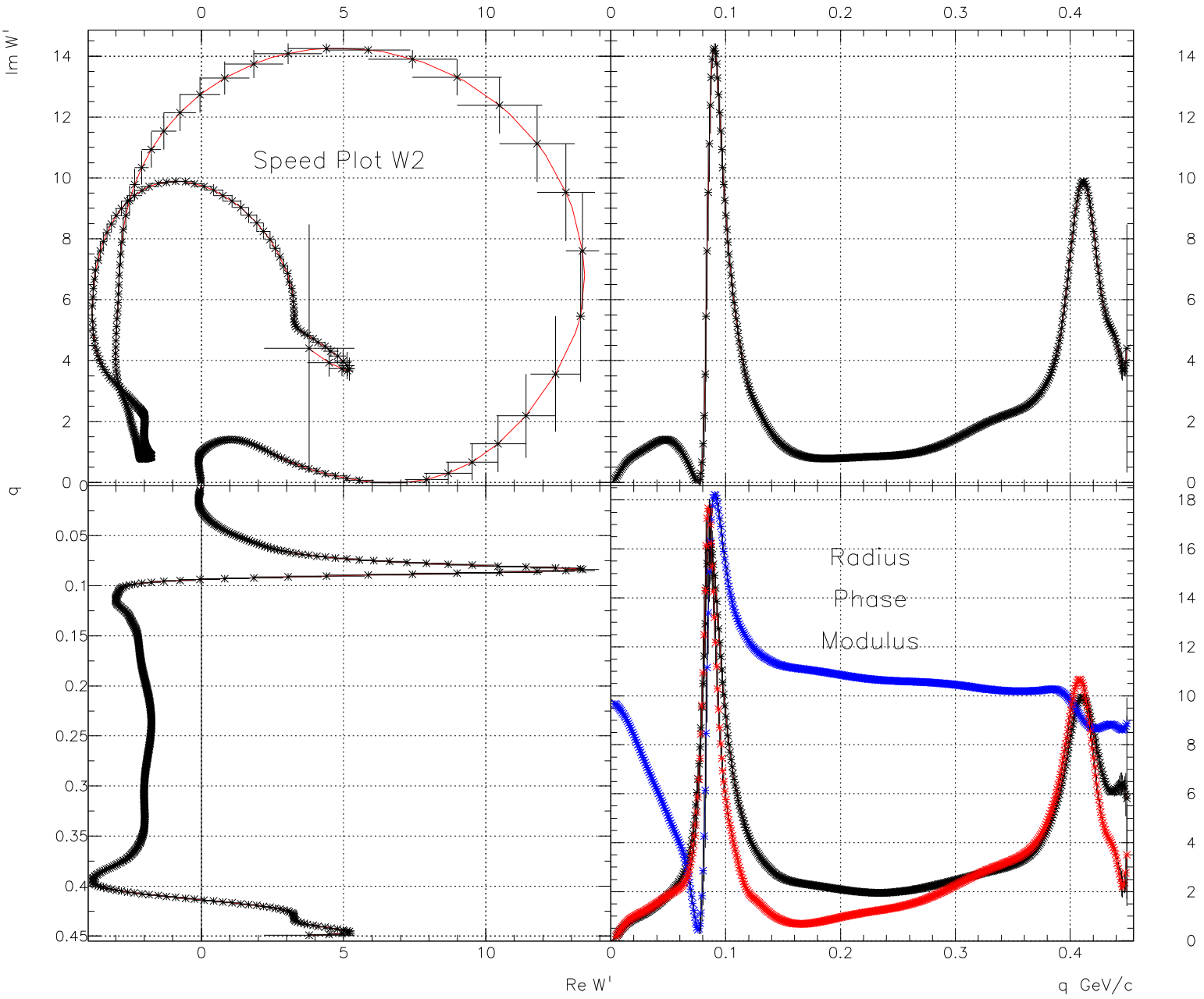

Figure 9: Zero Speed Plot for Trajectory W2.

3 Discrete phase shift analysis.

For the $\pi^+ p$ interaction a discrete phase shift analysis has been performed in the range $k = 0.077 - 0.725$ GeV/c at 77 different momenta. The main features of the analysis are :

1. We have used all data available from threshould up to 725 MeV/c.
2. To avoid an energy shifts between different data sets the interpolation technique was employed, parabolic or linear, depending on the data set.
3. Forward scattering amplitude was constrained iteratively by Pietarinen's technic.
4. The normalization were allowed to float according to experimental systematic uncertainty.
5. Angular scaling was applied to all data, based on the experimental Resolutions.
6. All observables were calculated taking into account experimental Acceptances.
7. Tromborg EM corrections have been used to extract the hadronic amplitudes.
8. There were no cut-off in angular momentum approaching the threshold. To stabilize the low energy behaviour we have used effective-range parametization based on the PWD results and the smoothness of the Zero trajectories. The maximal angular momentum was equal to 6 (H-wave approach, 11 partial waves).
9. Total inelastic cross sections on two pion production were used as additional constraint in the analysis.
10. The Analysis has an iterative nature and is not completed. There is plenty of room for improvements.

4 Results.

The Confidence Level of the analysis is 90÷100% depending on the energy. Only negligible number of the data points were eliminated with a $\chi^2 > 4$ due to inappropriate angular dependence.

Because of a huge amount of output information I limit myself only by slide show with a global results and some certain energy outputs.

Who are interested in more complete information on the data description may request it and we'll take it from the Helsinki Data Base in a few minutes online.

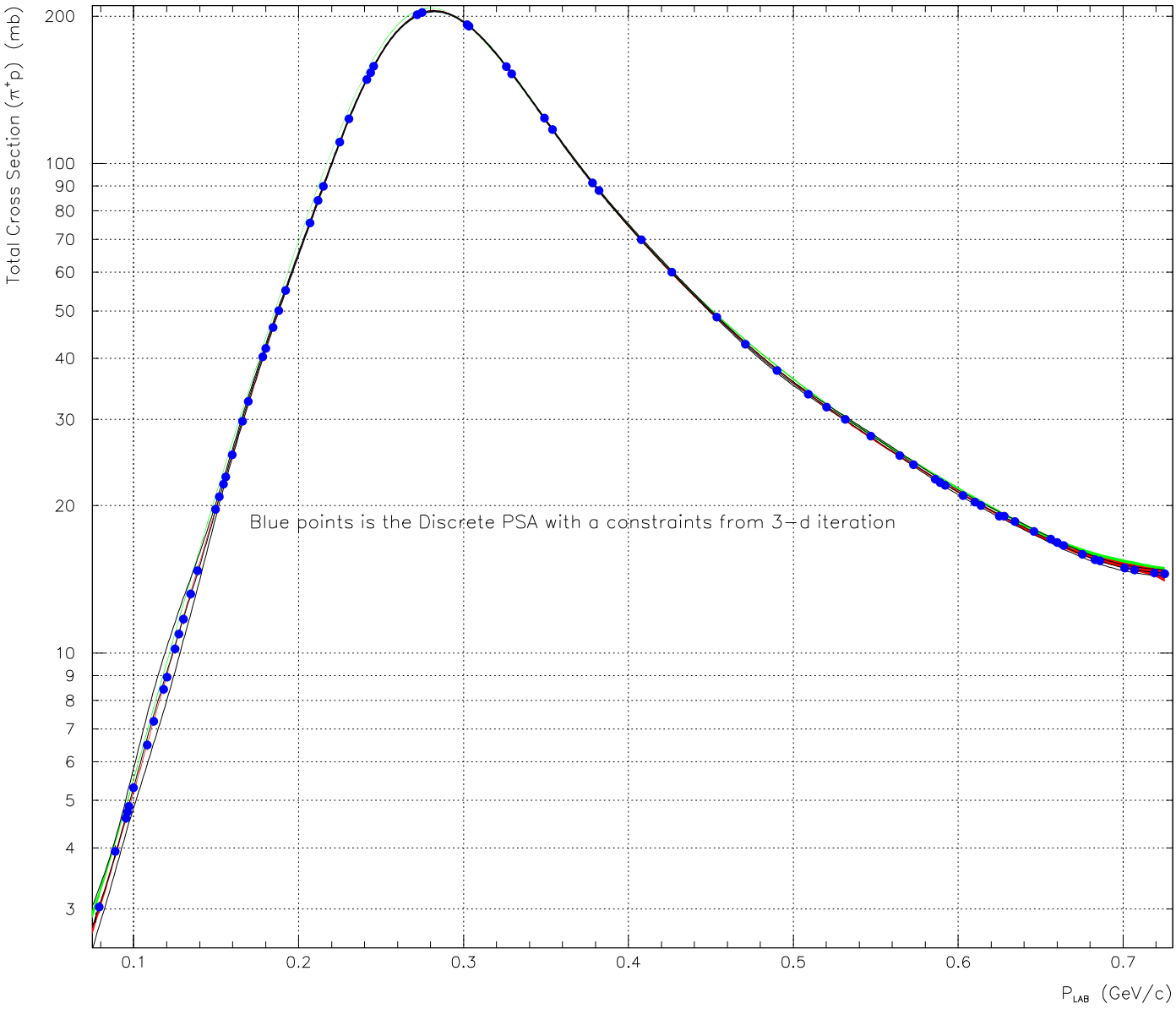

Figure 10: Total cross sections.

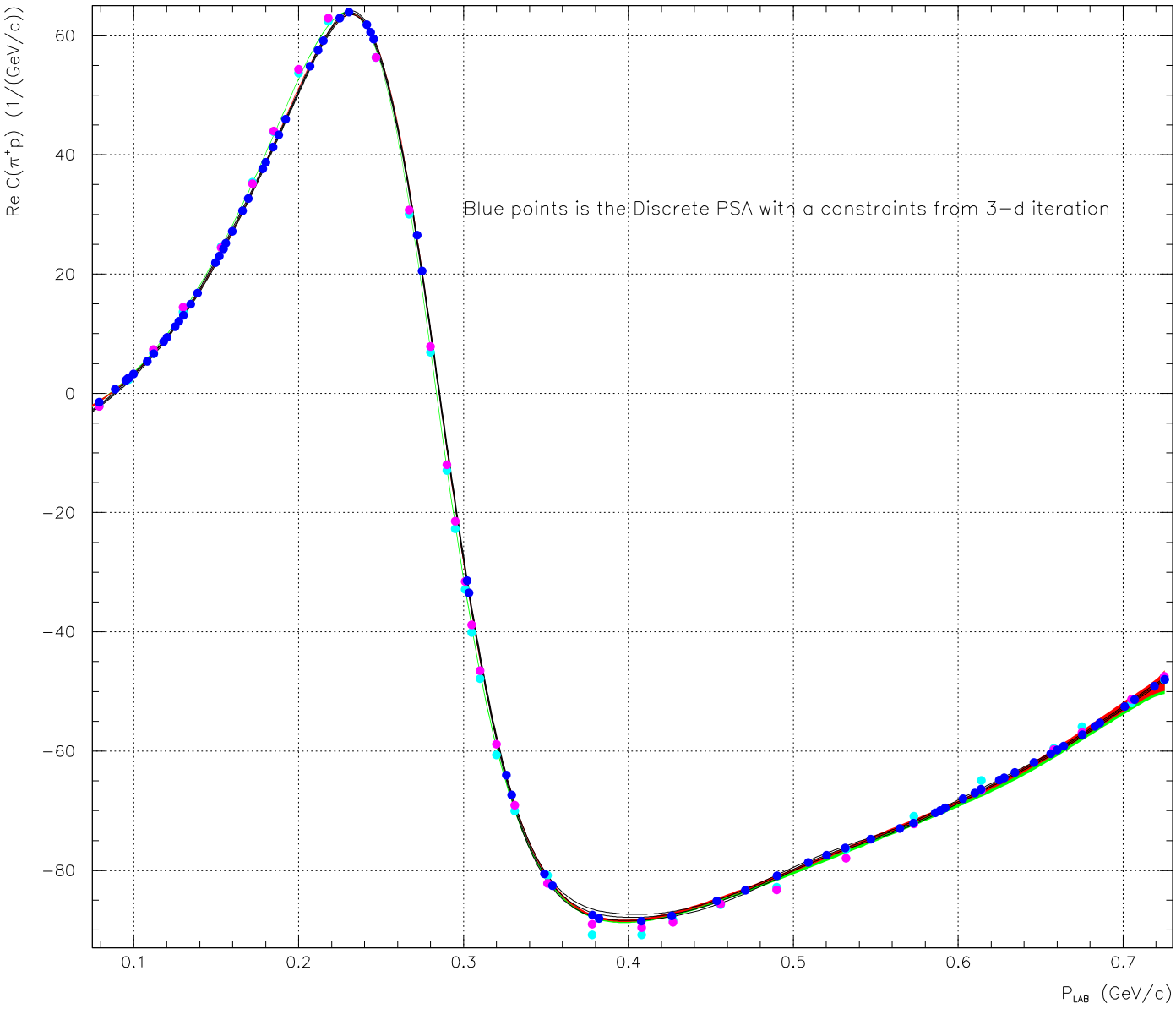

Figure 11: Real part for Forward scattering amplitude.

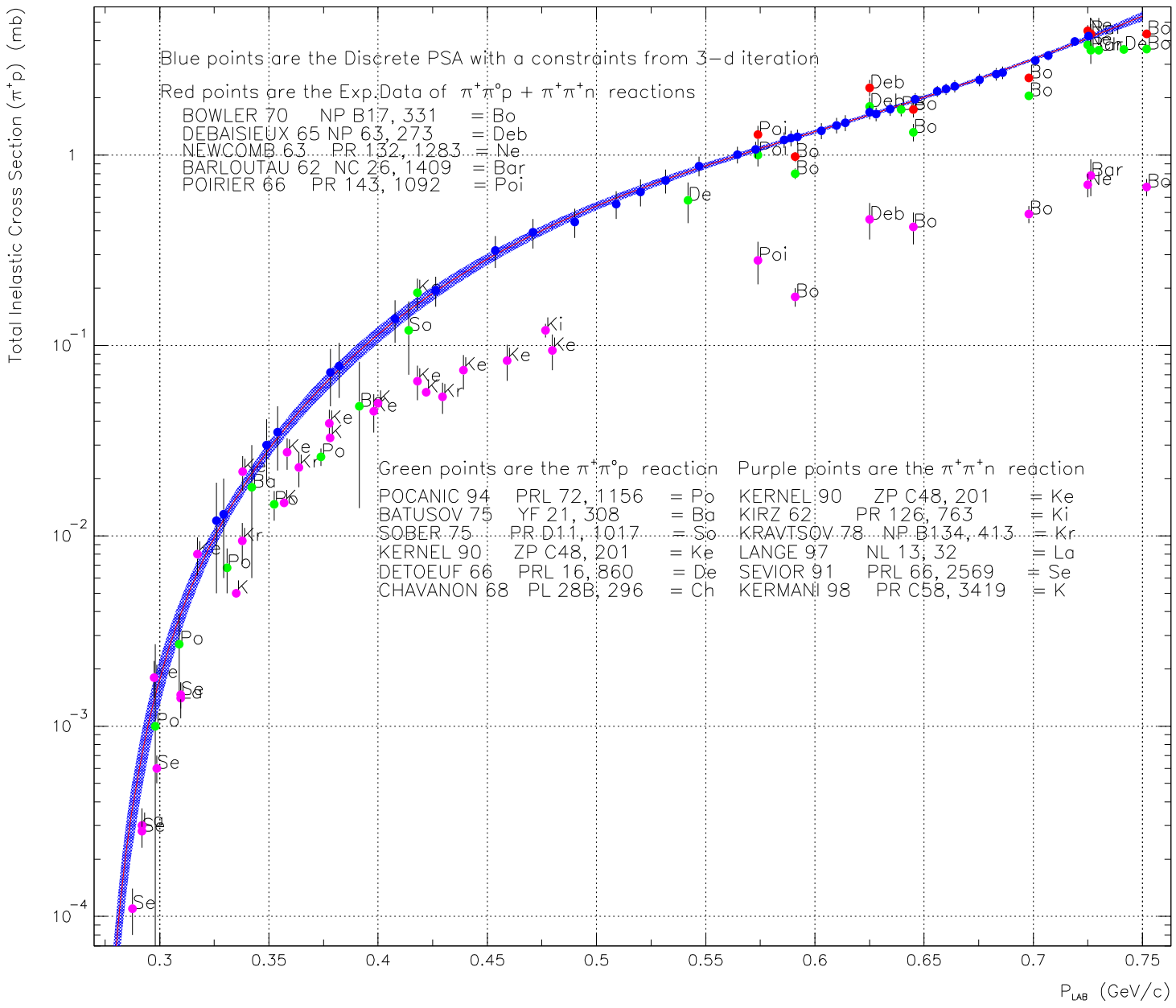

Figure 12: Total Inelastic cross sections.

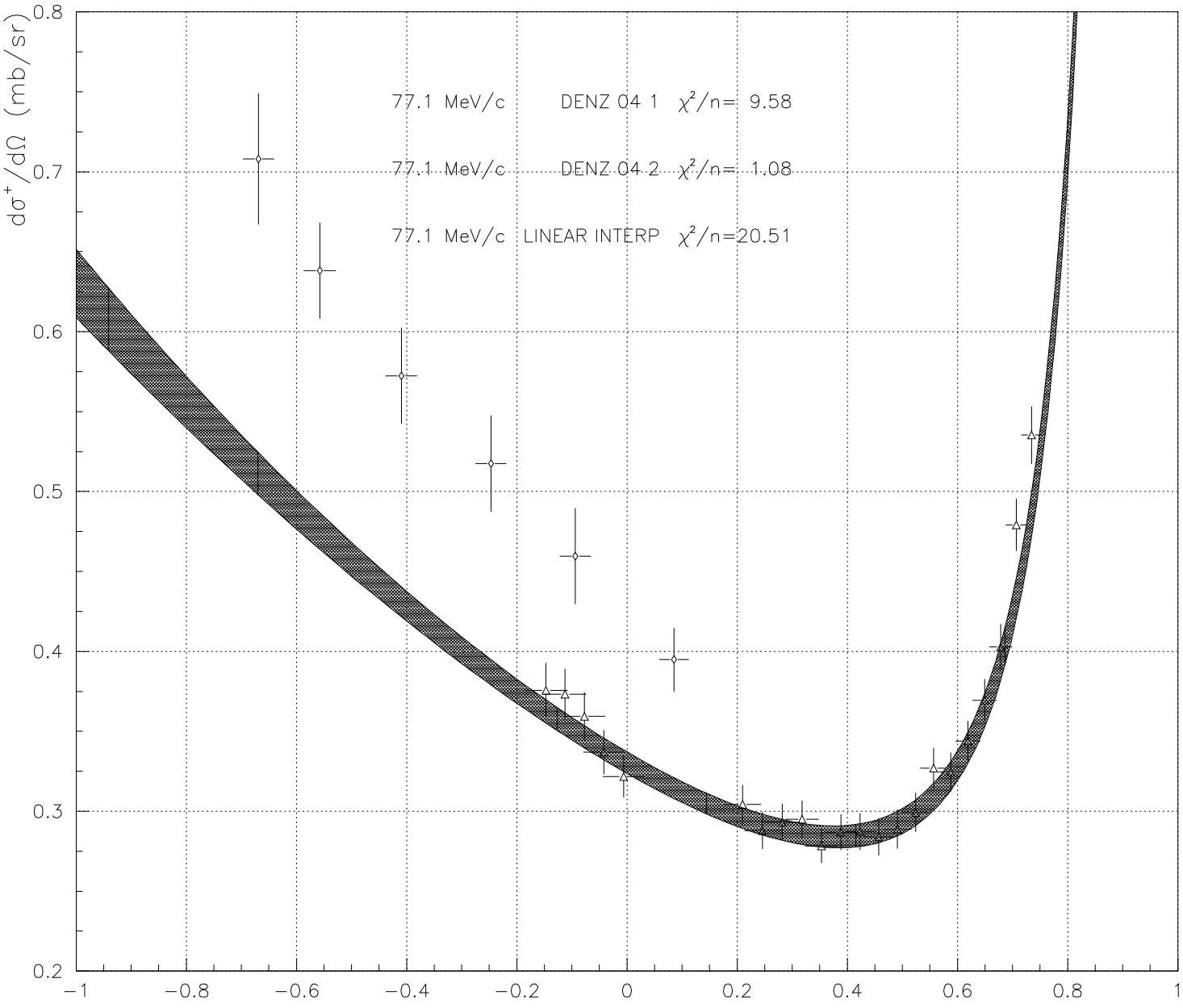

Figure 13: 77.1 MeV/c Original Dentz-2004 and Bertine-1976.

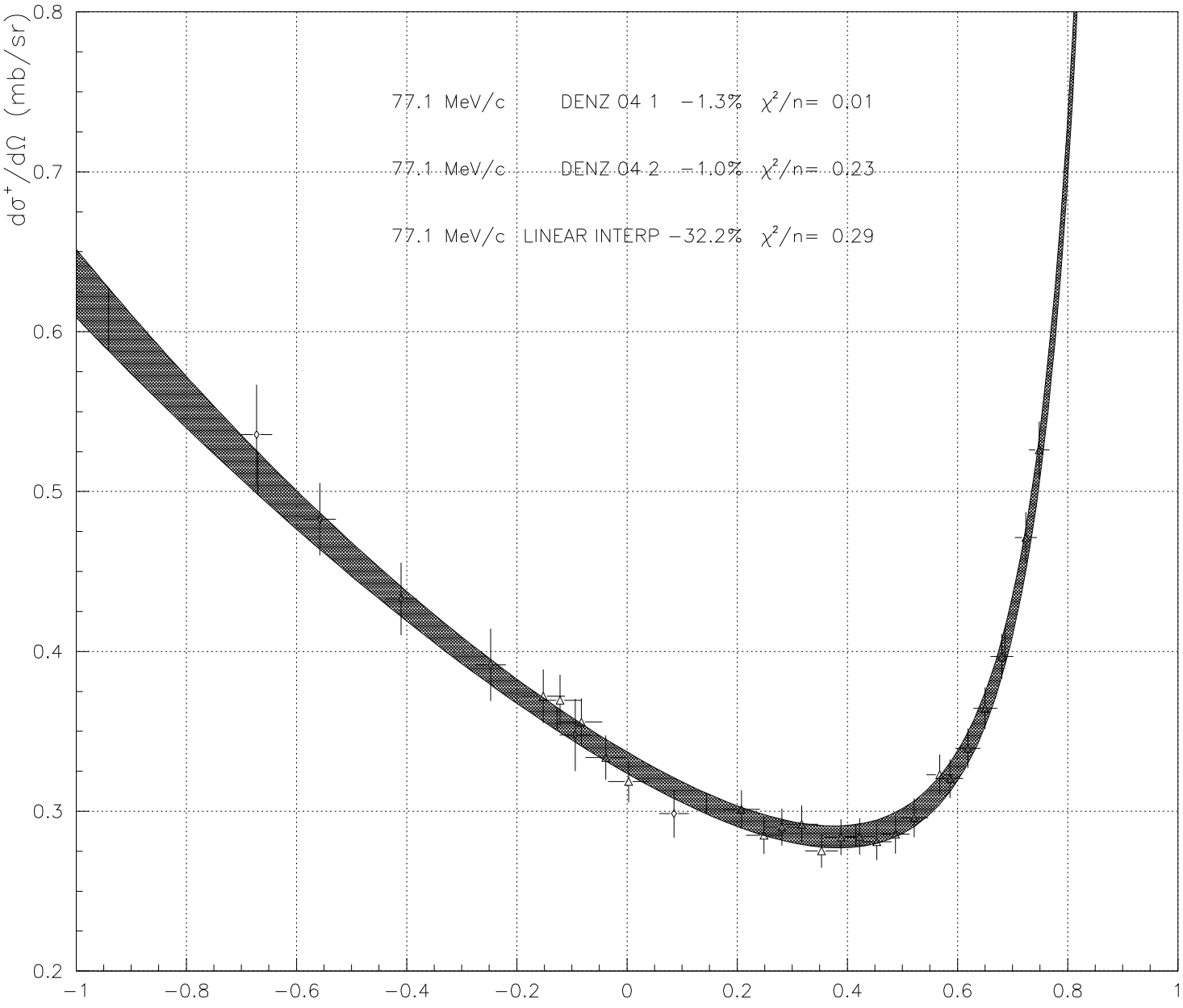

Figure 14: 77.1 MeV/c Corrected Dentz-2004 and Bertine-1976.

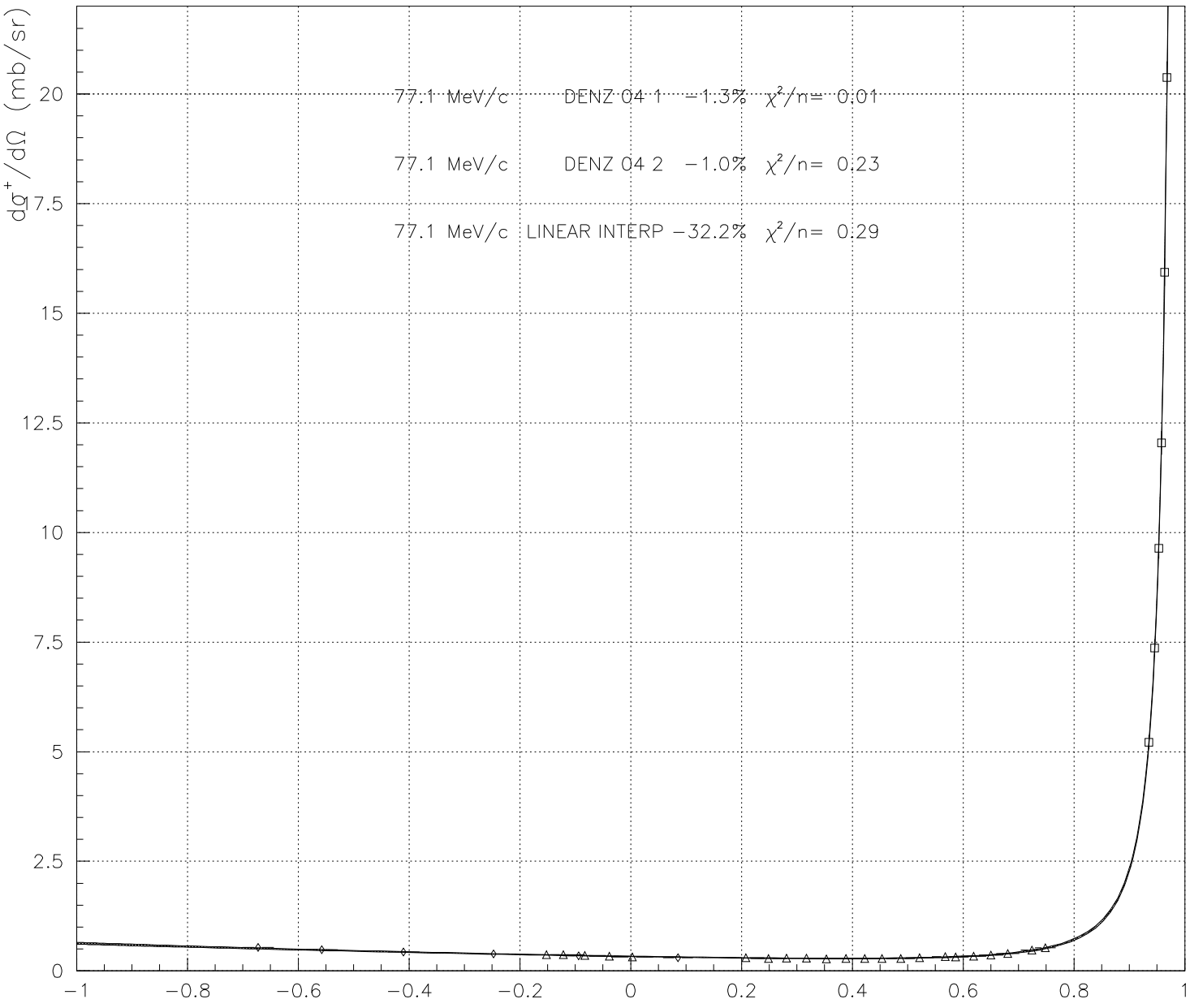

Figure 15: 77.1 MeV/c Corrected Dentz-2004 and Bertine-1976.

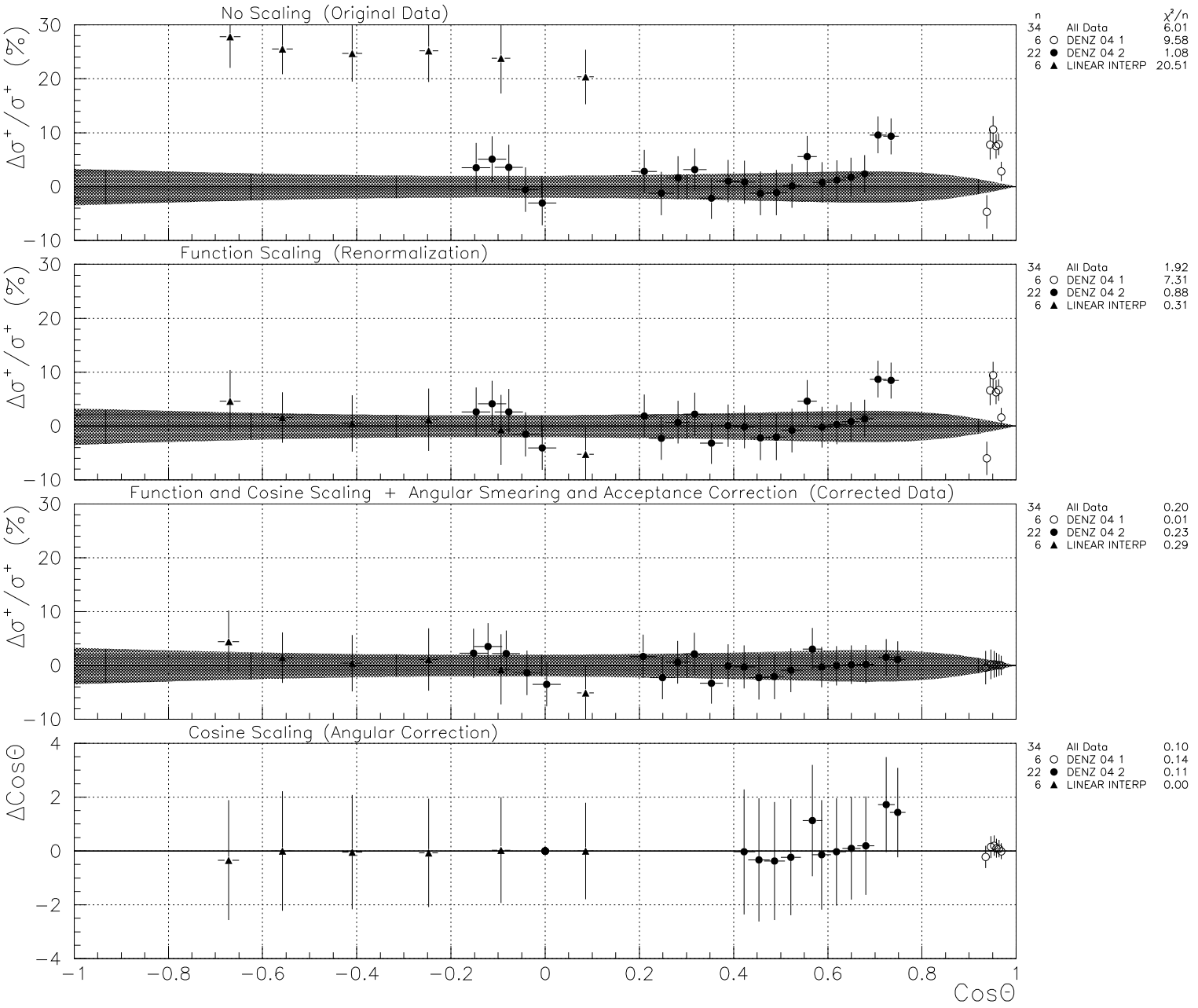

Figure 16: 77.1 MeV/c Deviation plots.

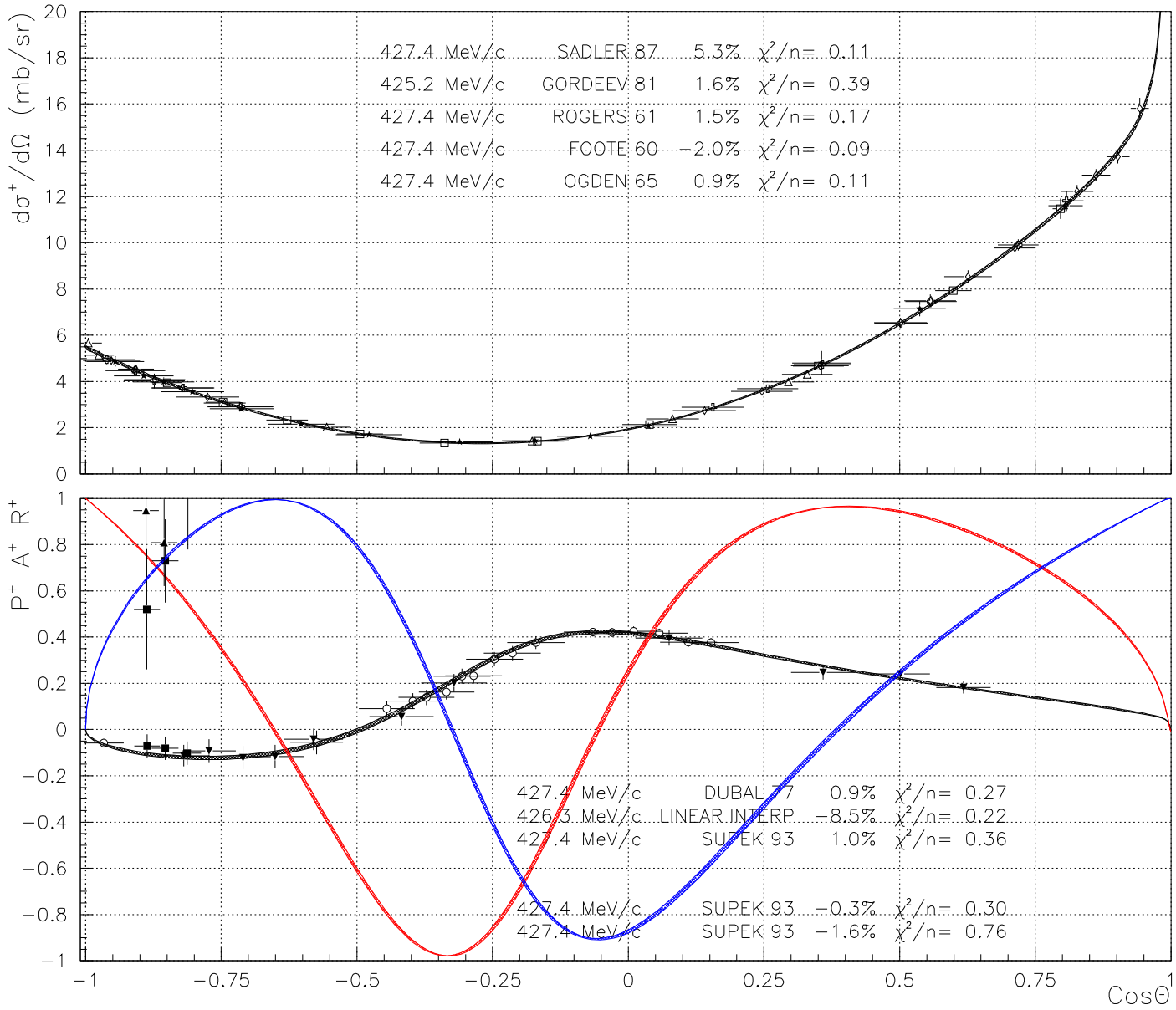

Figure 17: 426.3 MeV/c Corrected data.

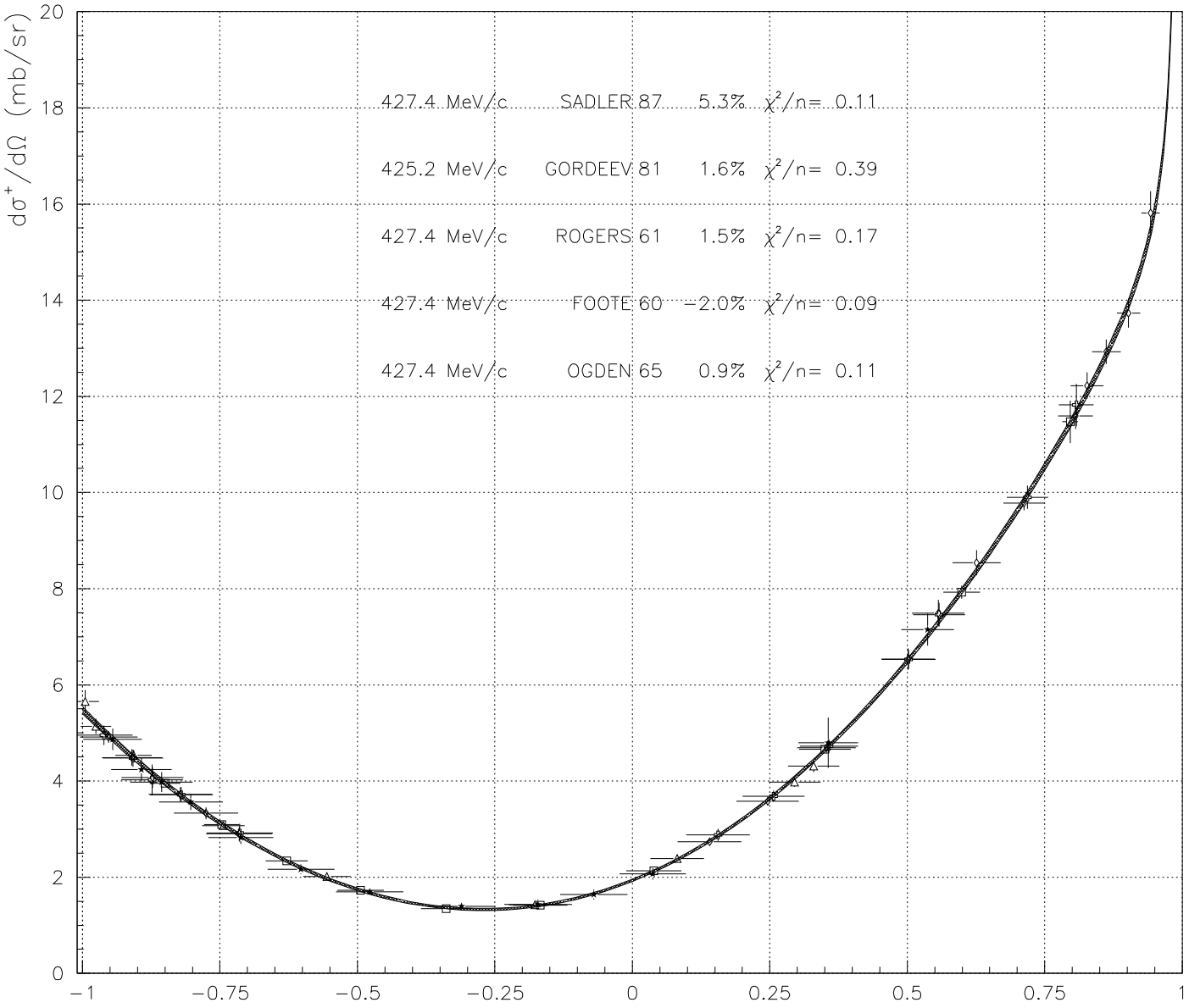

Figure 18: 426.3 MeV/c Corrected Sadler-1987, Gordeev-1981, Rogers-1961, Foote-1960 and Ogden-1965.

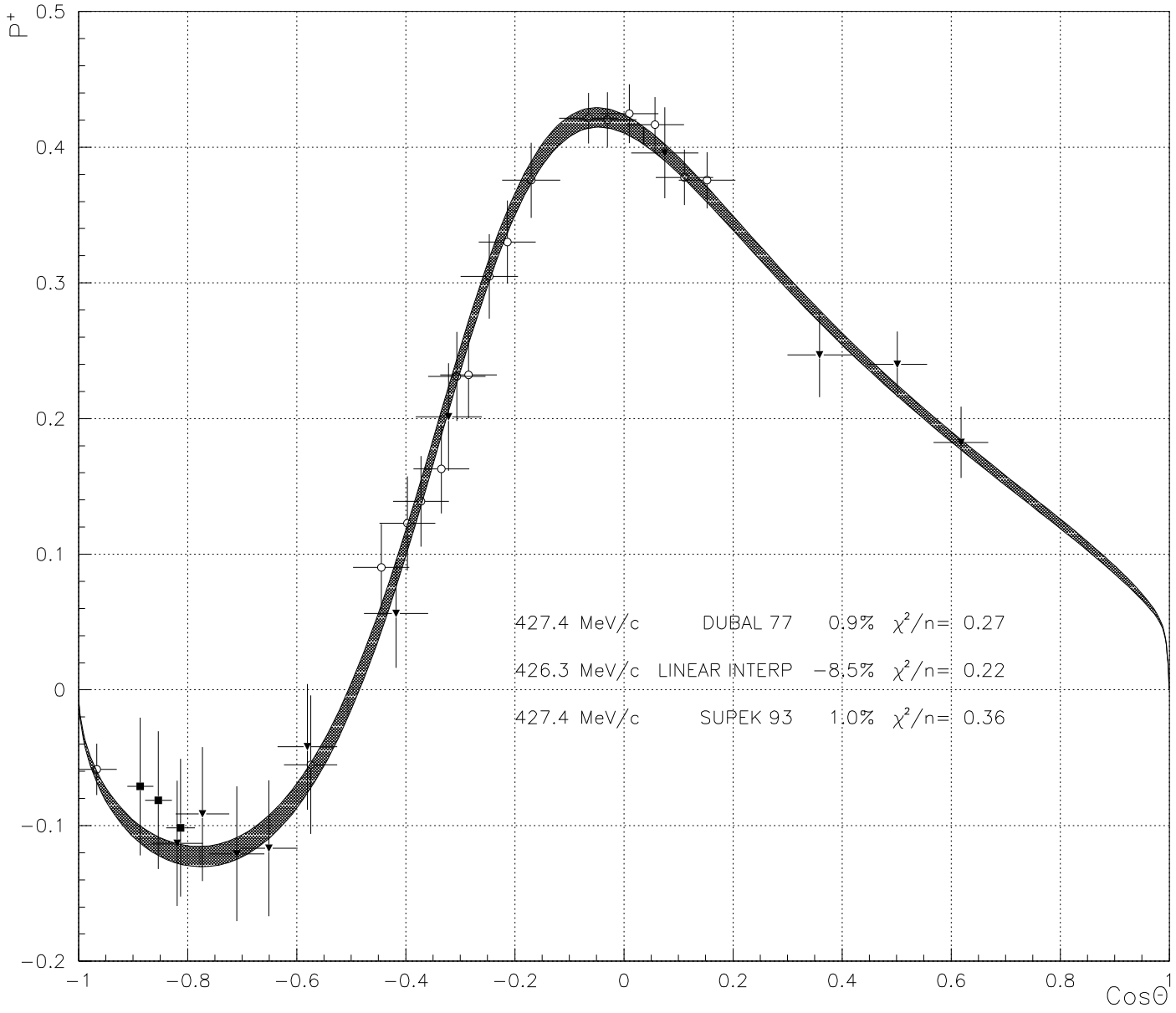

Figure 19: 426.3 MeV/c Corrected Dubal-1977, Gordeev-1981, Gorn-1973, and Supek-1993.

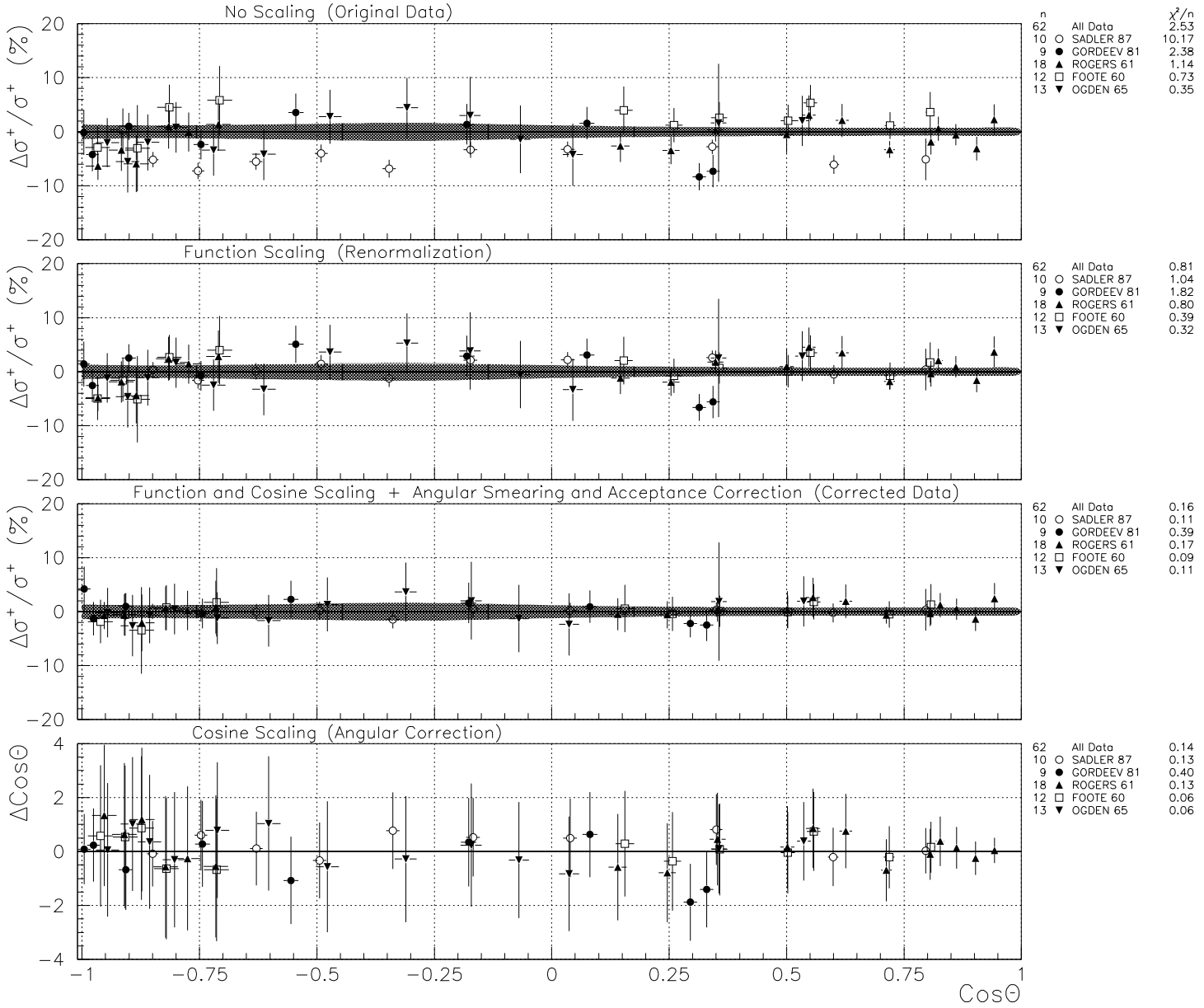

Figure 20: 426.3 MeV/c Deviation plots for differential cross sections.

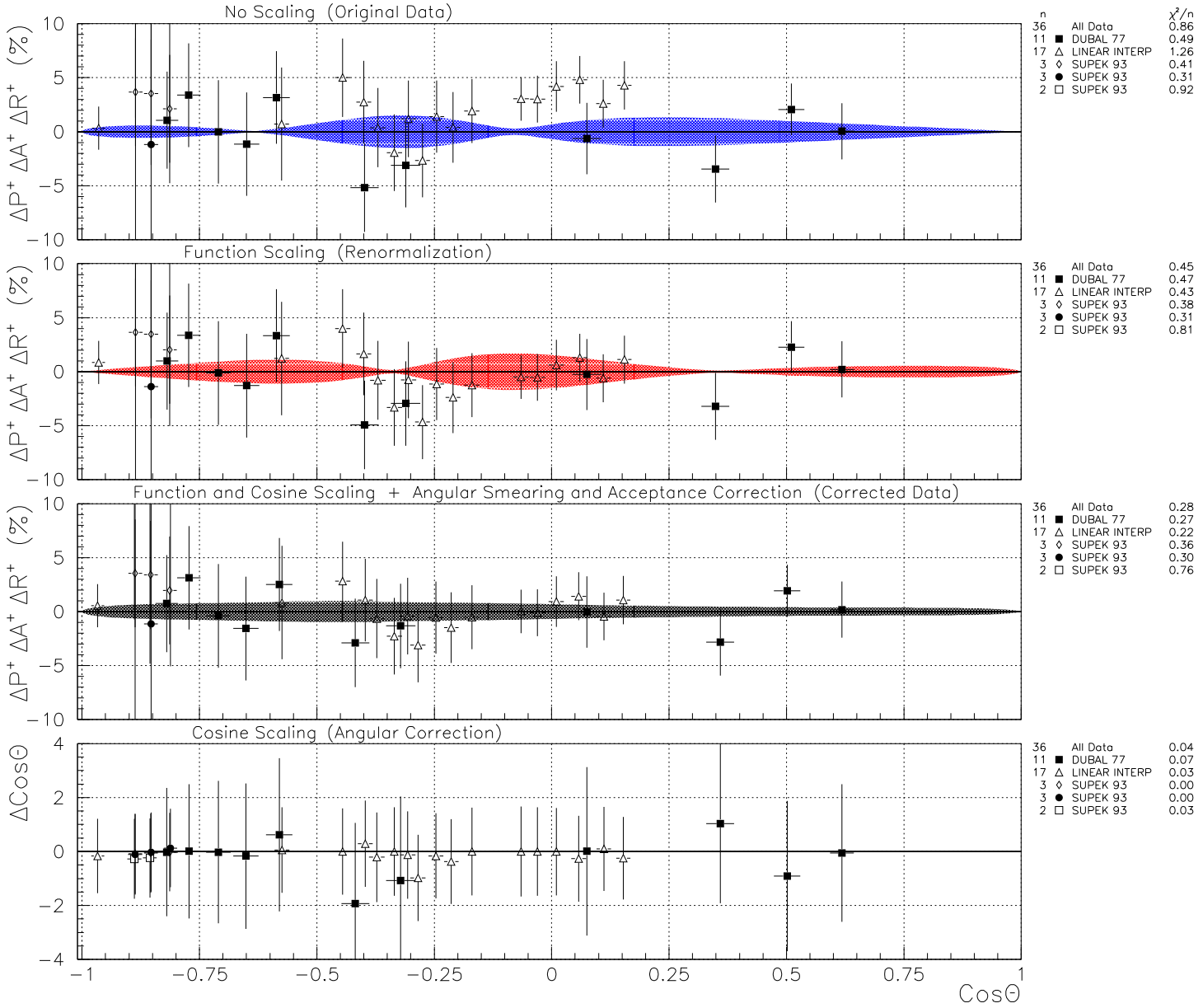

Figure 21: 426.3 MeV/c Deviation plots for P,R and A.

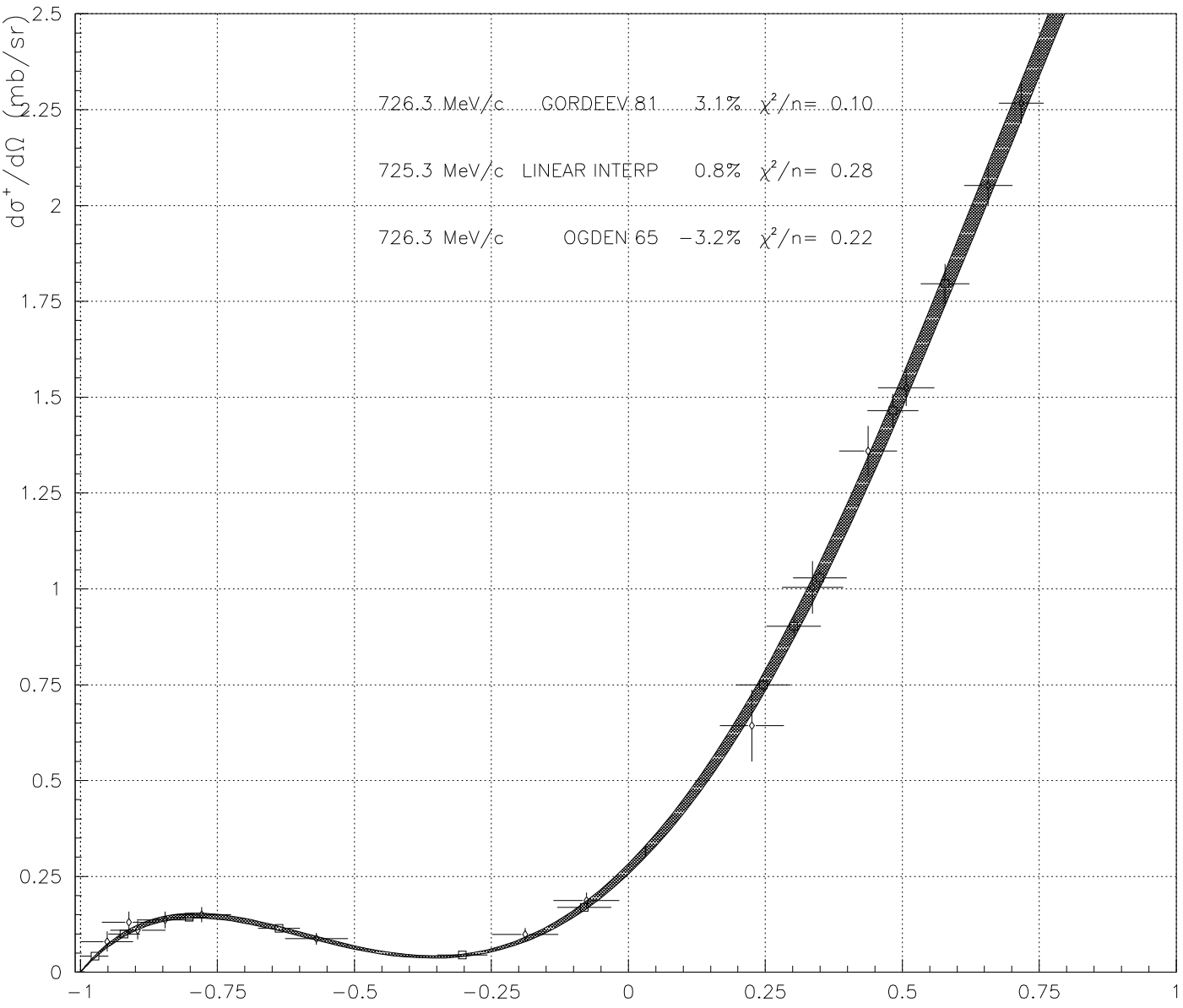

Figure 22: 725.3 MeV/c Corrected Gordeev-1981, Rothschild-1972 and Ogden-1965.

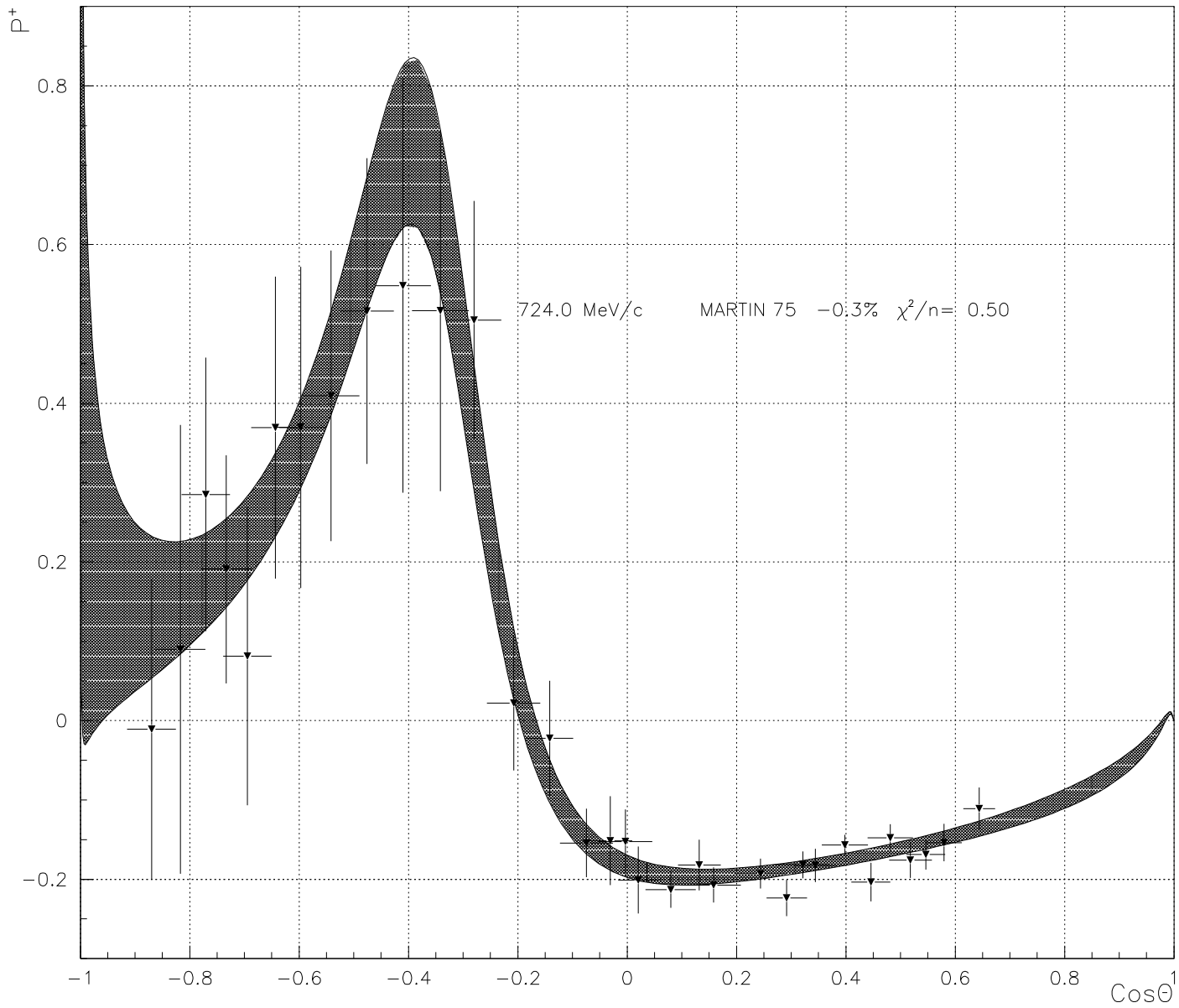

Figure 23: 725.3 MeV/c Corrected Martin-1975.

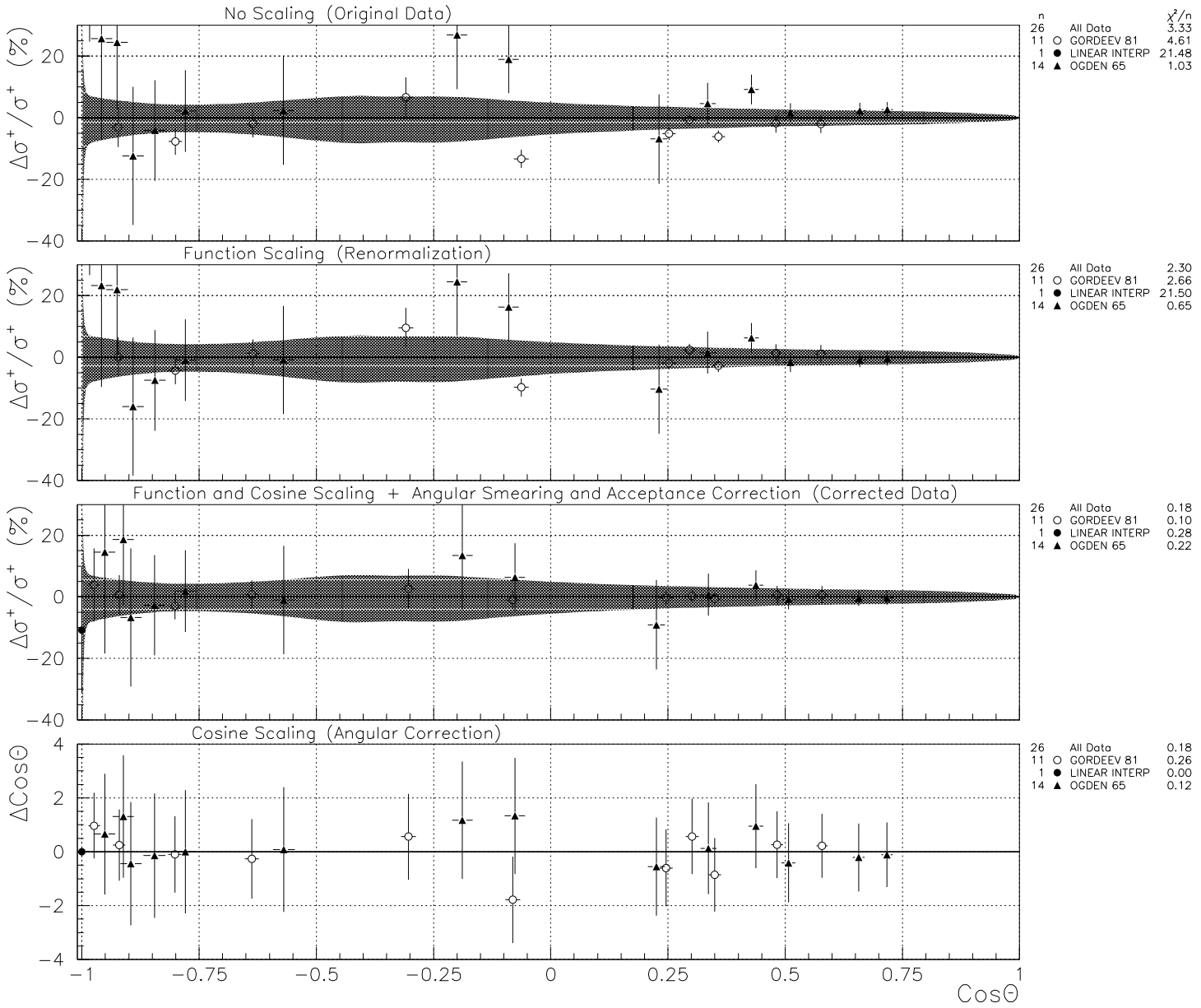

Figure 24: 725.3 MeV/c Deviation plots for differential cross sections.

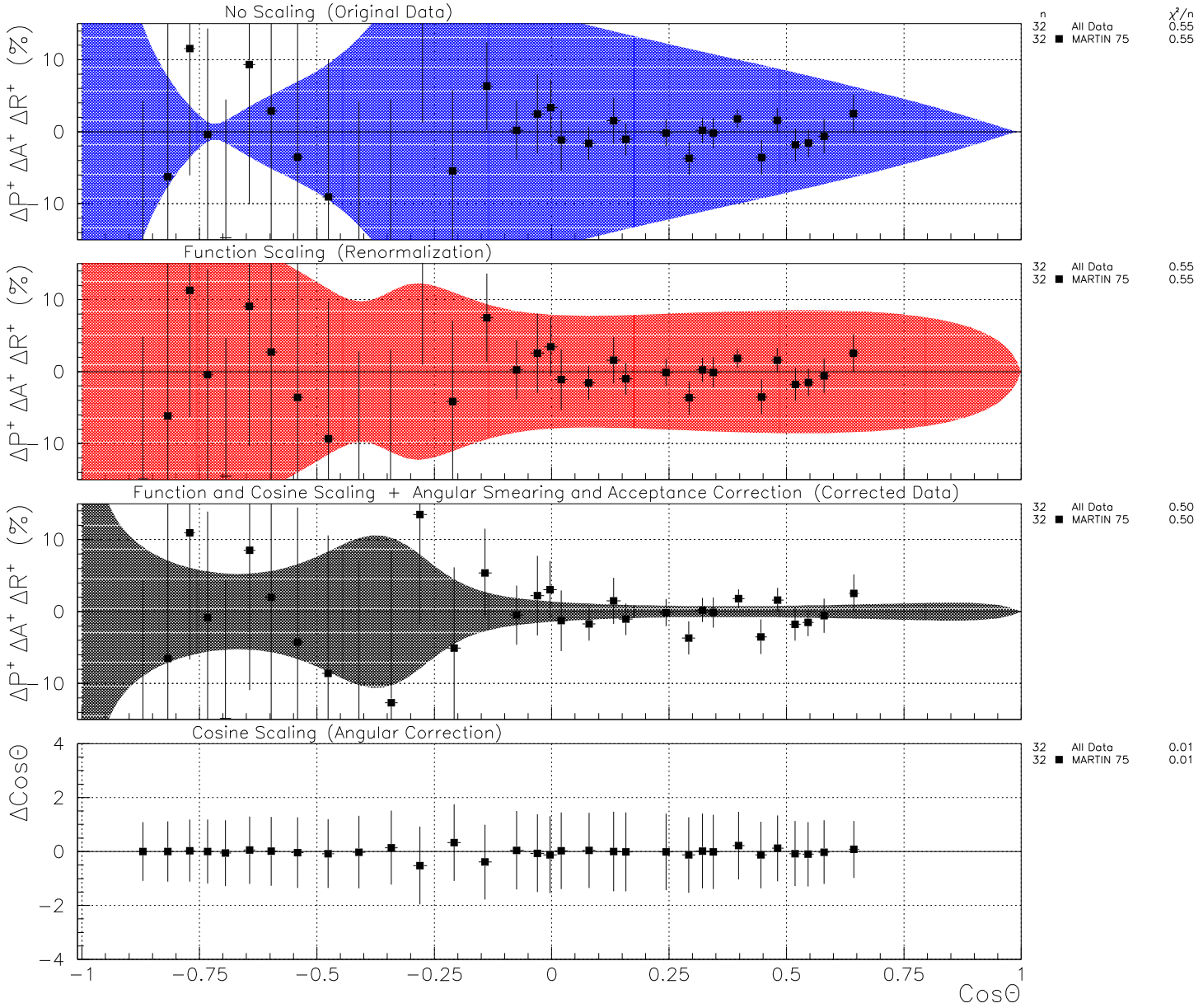

Figure 25: 725.3 MeV/c Deviation plots for polarization.

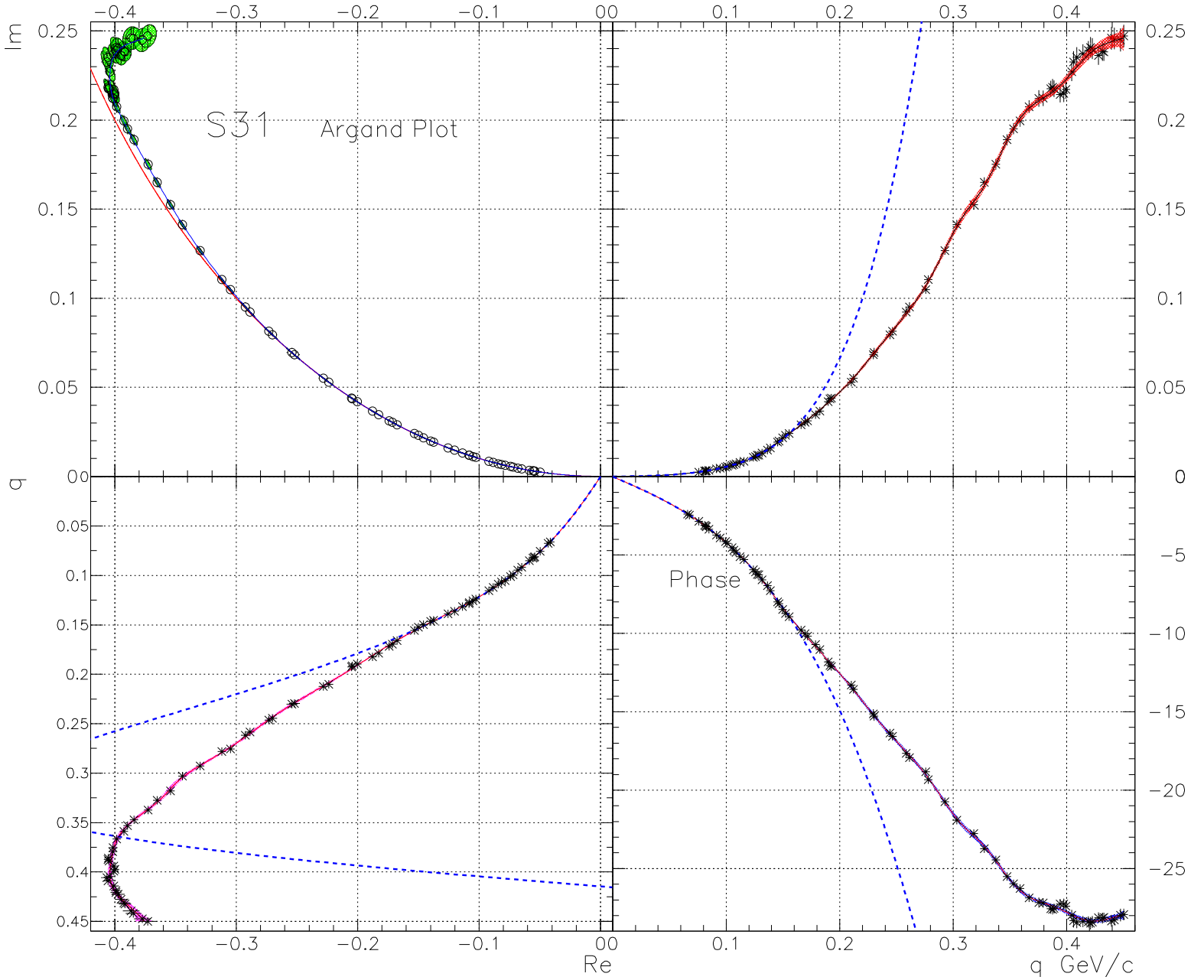

Figure 26: Argand plot for $S31$-amplitude from discrete phase shift analysis and effective range approximation.

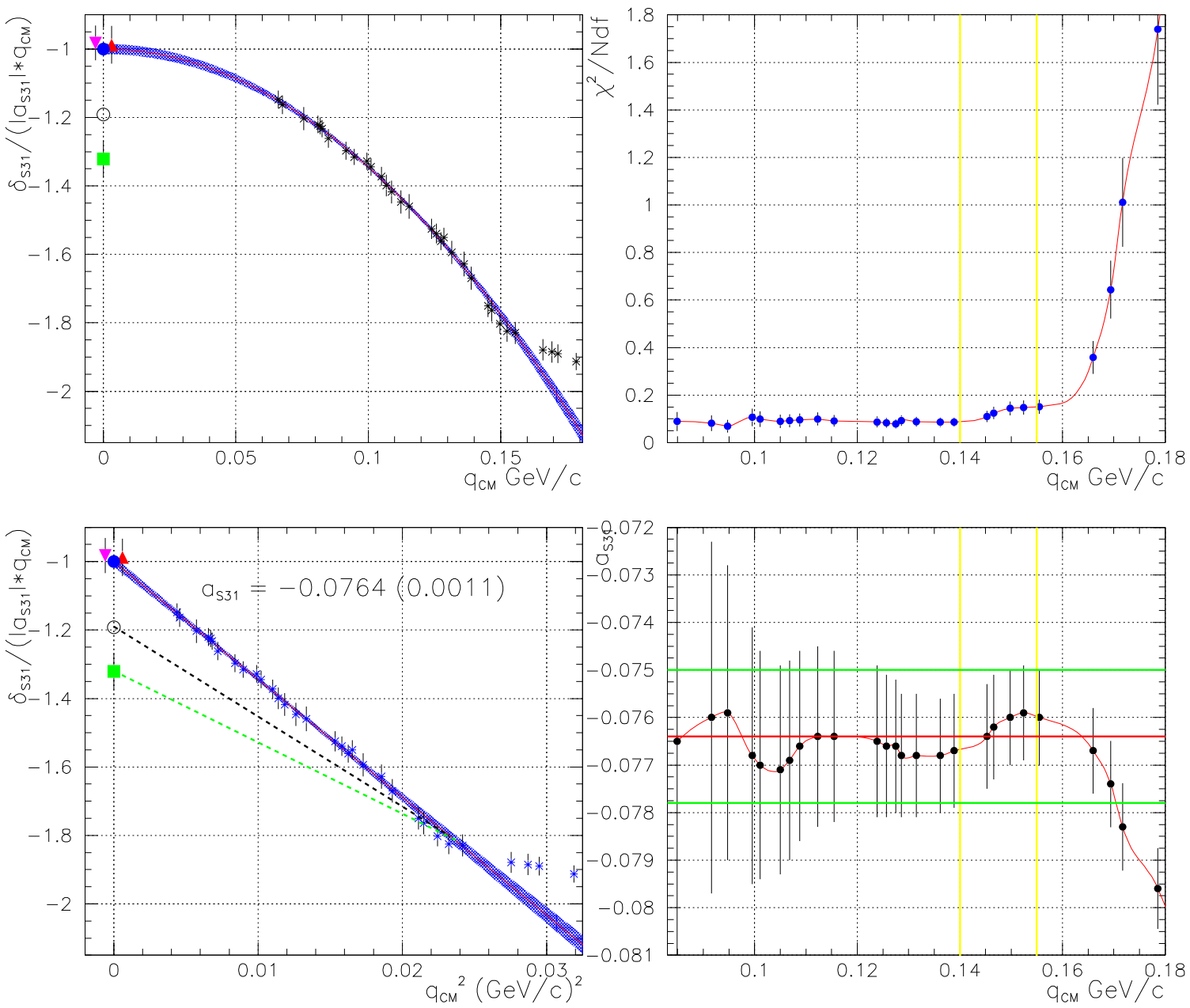

Figure 27: Effective range parametrization and estimation of the energy interval validity.

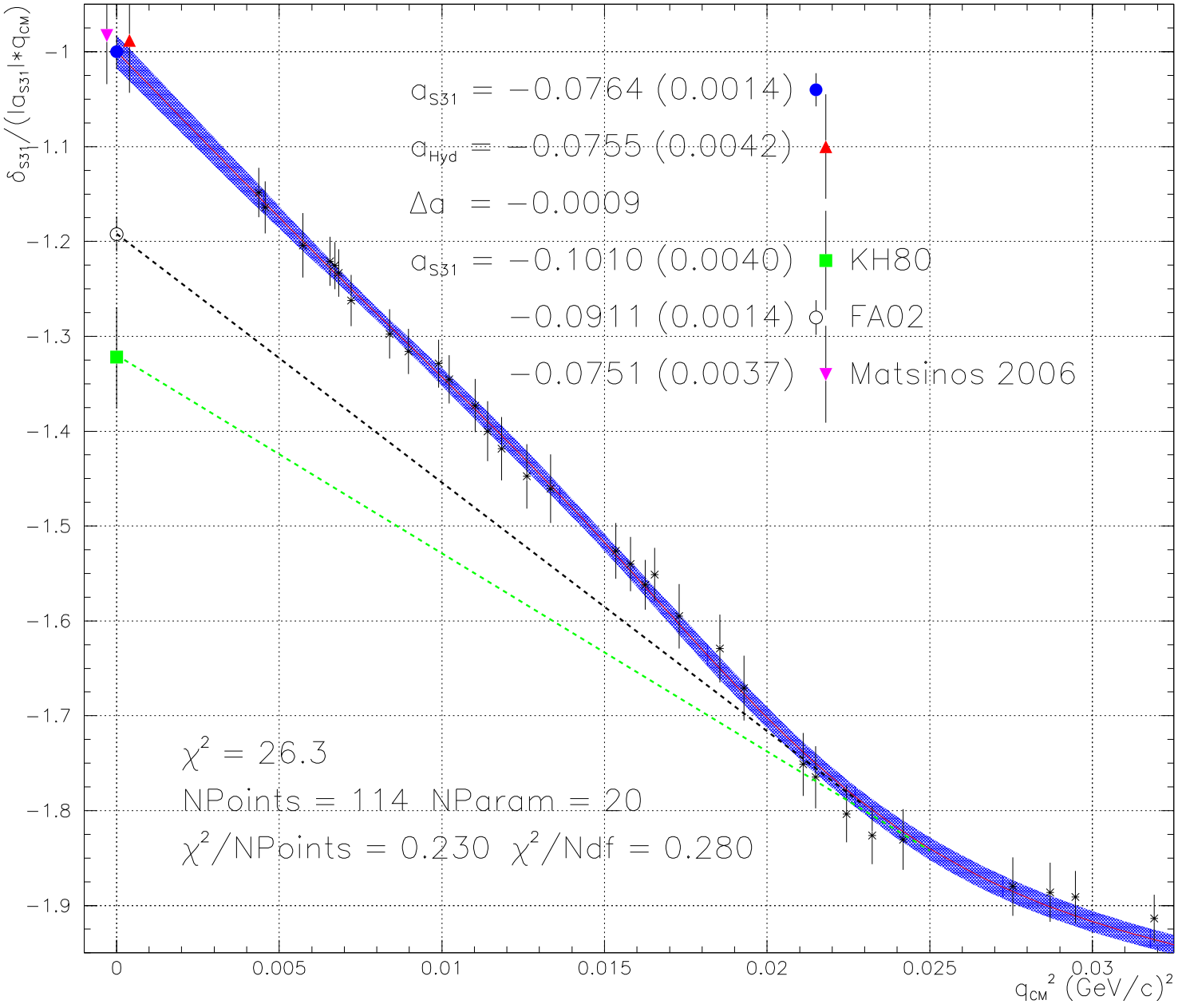

Figure 28: Result of the multy-parameter $S31$-amplidute parametization in the whole energy interval. The phase shift δ_{S31} normalized with $|a_{S31}|\,q$ as a function of the q^2. Relative error of the scattering length is $\Delta a_{S31}/a_{S31} \simeq \pm 2\%$. There is good agreement with hydrogen and Matsinos results, but dramatical difference compare to KH80, $32 \pm 6\%$, and Arndt, $19 \pm 3\%$, solutions.

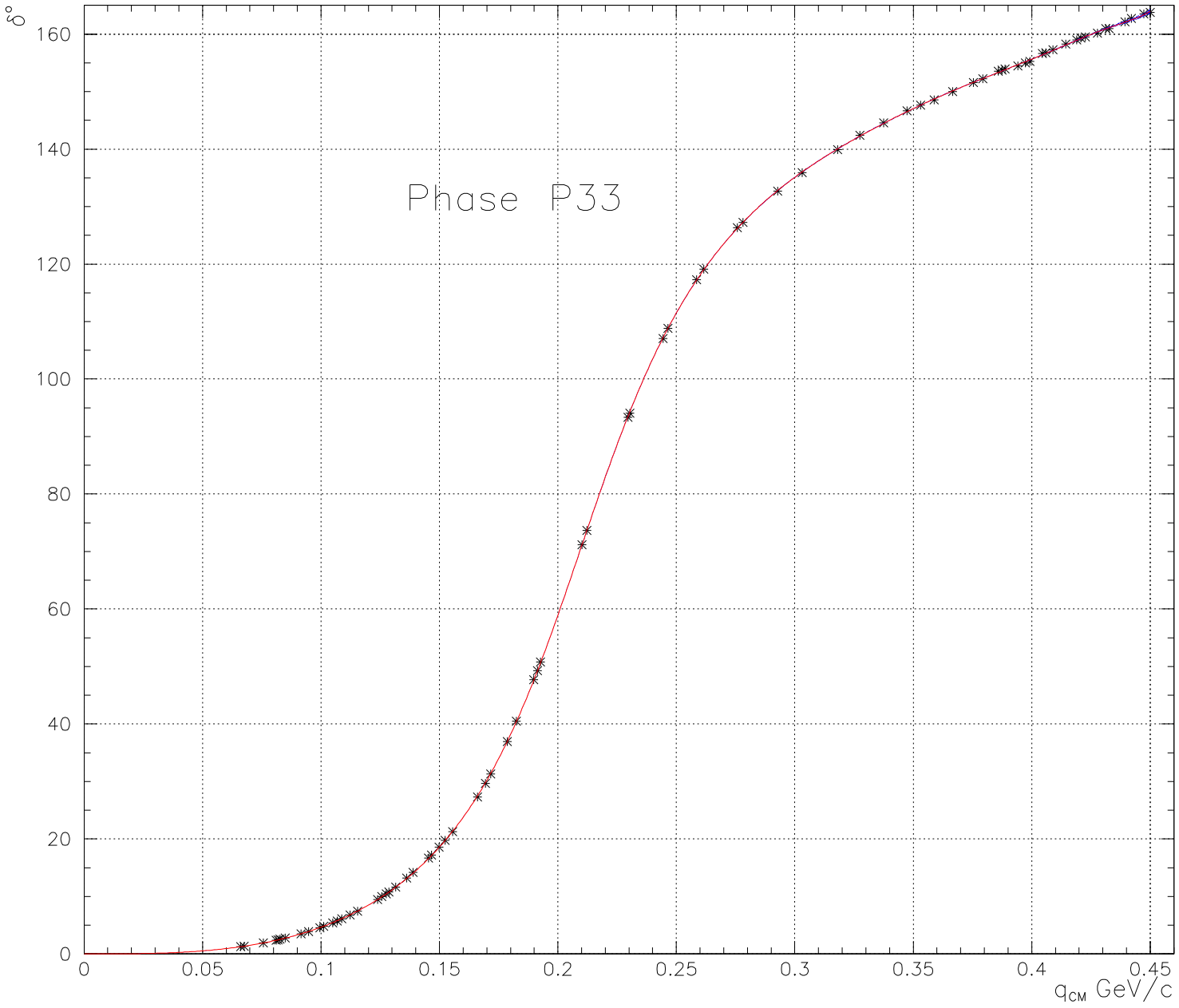

Figure 29: P33 Phase Shift.

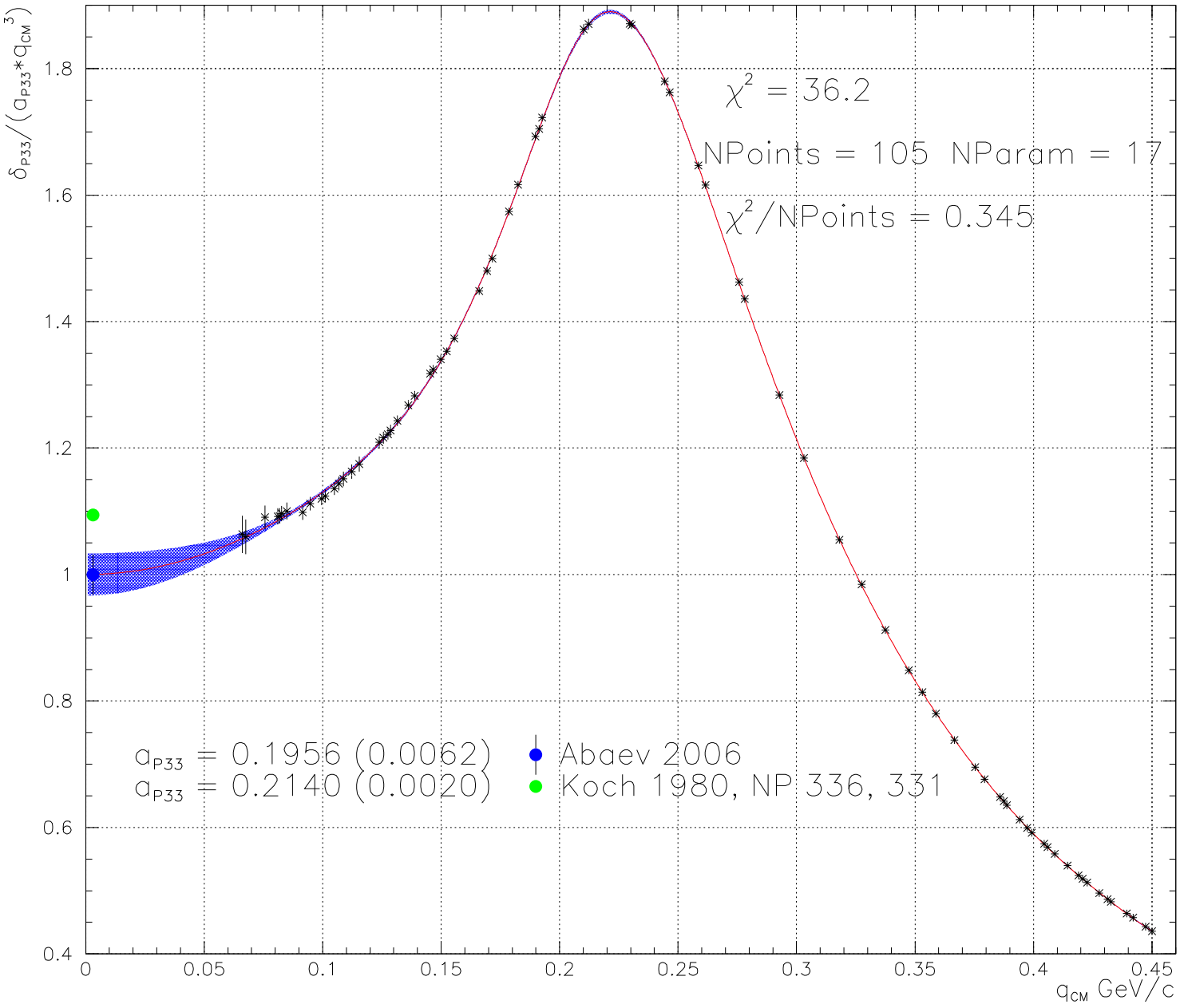

Figure 30: Renormalized P33 Phase Shift as a function of q .

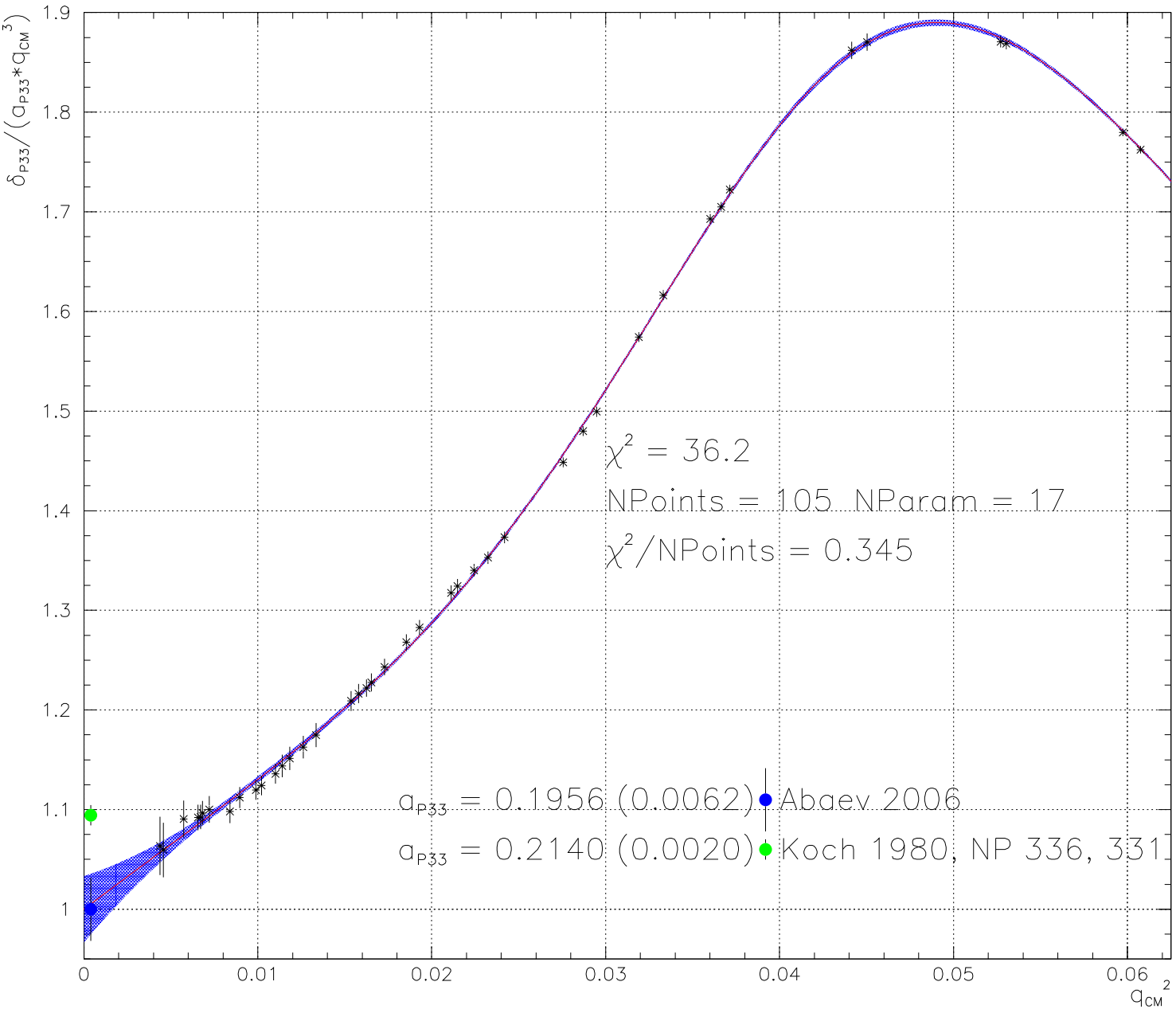

Figure 31: Renormalized P33 Phase Shift as a function of q^2 .

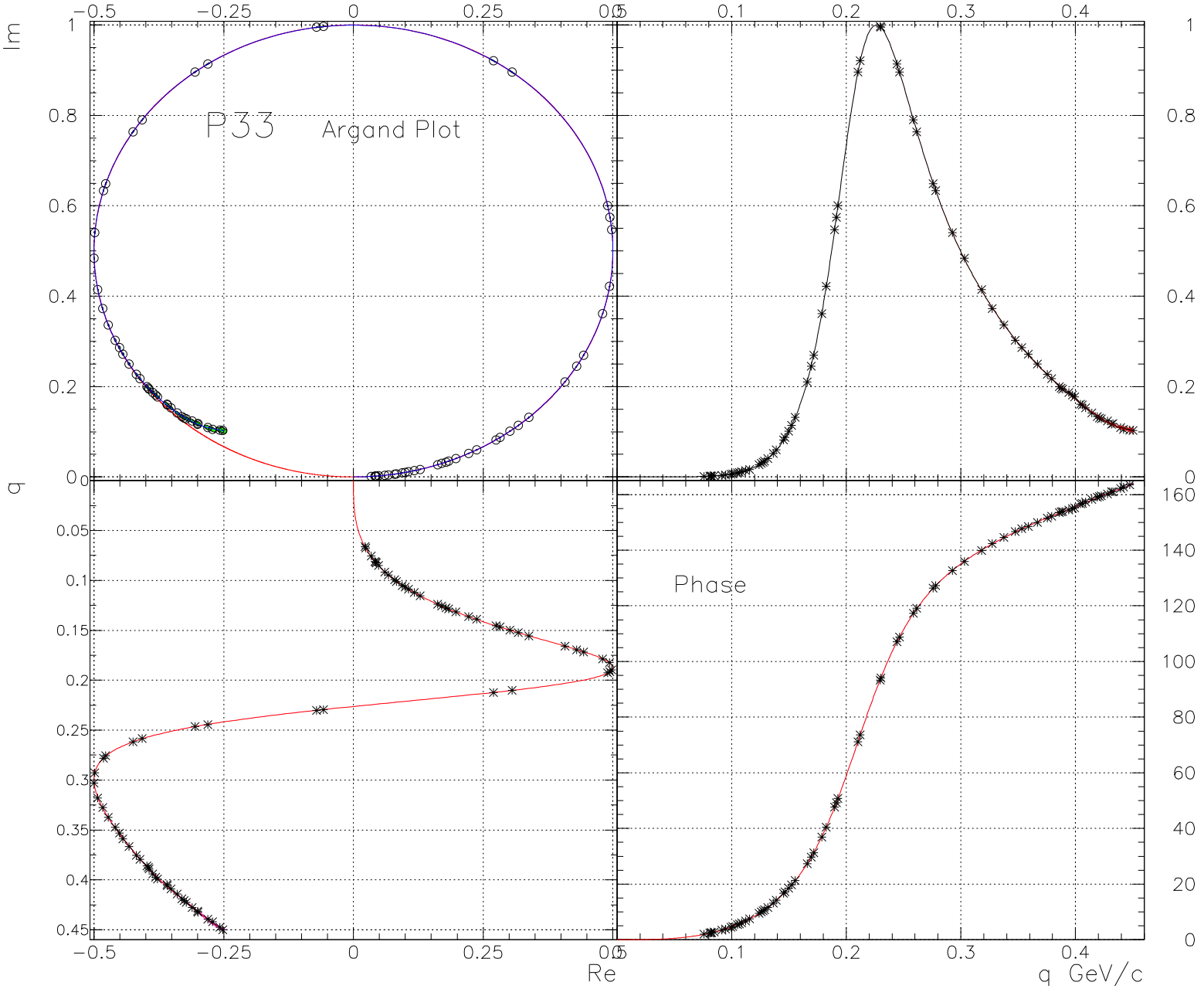

Figure 32: P33 Argand Plot.

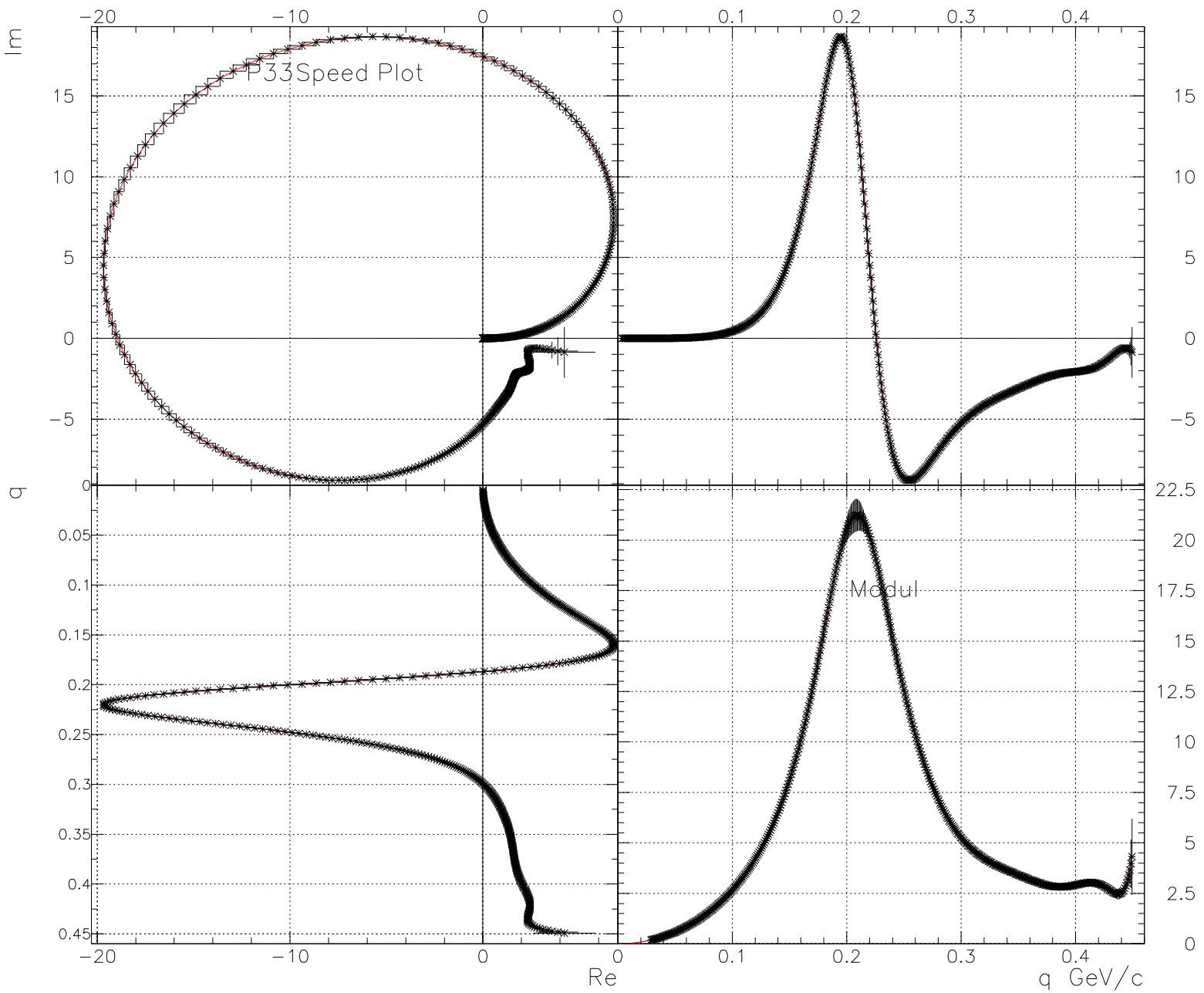

Figure 33: P33 Speed Plot.

5 Conclusions.

1. Our discrete phase shift analysis is still in progress as an iterative procedure and the results are preliminary.

2. New Code proved strength and reliability. We did not find weighty inconsistency in the Data Base.

3. There is room for code's impovement and it is under the way both theoretically and practically.

4. The a_{S31}-wave scattering length appeared to be stable at this stage and hopefully would not be changed outside the error bars.